

# The Potts-Tutte Polynomial and Some Connections between Graph Theory and Statistical Mechanics

Robert Shrock

C. N. Yang Institute for Theoretical Physics and Department of Physics and Astronomy,  
Stony Brook University

Conference on Interplay between statistical mechanics, graph theory, computational complexity and holomorphic dynamics,  
June 10-11, 2021

# Outline

- Potts model in statistical mechanics and equivalence with Tutte polynomial in graph theory
- Chromatic polynomials and ground state entropy of Potts antiferromagnet
- Zeros of chromatic and Potts/Tutte polynomials and their accumulation sets as  $n \rightarrow \infty$
- Potts model on hierarchical family of graphs: Diamond hierarchical lattice
- Some open problems and directions for future research
- Conclusions

This includes work with V. Matveev, S.-H. Tsai, S.-C. Chang, and R. Roeder

# Potts Model Partition Function and Tutte Polynomial

The Potts model has long been of interest in statistical physics and is closely related to the Tutte (also called Tutte-Whitney) polynomial in mathematical graph theory.

The physics context: statistical physics deals with properties of many-body systems. The description of such systems uses a specified form of the interaction between the dynamical variables. An example is magnetic systems, where the dynamical variables are spins located at sites of a lattice. These interact with each other by an energy function, the Hamiltonian  $\mathcal{H}$ . A common limit is  $n \rightarrow \infty$  where  $n$  is the number of sites. In practice, a typical number in experiments is Avogadro's number,  $N_{Av} = 6.02 \times 10^{23}$  per mole.

Consider the general case of a graph  $G = (V, E)$ , where  $V$  is the set of vertices (sites) and  $E$  is the set of edges (bonds). Denote  $n = n(G) = |V|$  as the number of vertices,  $e(G) = |E|$  as the number of edges,  $k(G)$  as the number of connected components, and  $c(G)$  as the number of linearly independent circuits in  $G$ .

In statistical physics, one considers a many-body system in thermal equilibrium at a temperature  $T$ . Let  $\beta = 1/(k_B T)$ , where  $k_B = 1.38 \times 10^{-23}$  J/K is the Boltzmann constant.

In its physics formulation, the Potts model describes a system with classical spins  $\sigma_i$  at vertices of a lattice graph  $G$ , each of which can take on any of  $q$  different values in  $\{1, 2, \dots, q\}$ . The Hamiltonian of the Potts model is

$$\mathcal{H} = -J \sum_{e_{ij}} \delta_{\sigma_i \sigma_j}$$

where  $\delta_{\sigma_i \sigma_j}$  is the Kronecker delta function and  $e_{ij}$  is an edge in  $G$  connecting vertices  $i$  and  $j$ . The couplings  $J > 0$  and  $J < 0$  favor parallel and antiparallel neighboring spins, and thus ferromagnetic (FM) and antiferromagnetic (AFM) spin ordering.

A useful function in the description of this system is the partition function:

$$Z = \sum_{\{\sigma_i\}} e^{-\beta \mathcal{H}} = \sum_{\{\sigma_i\}} e^{K \sum_{e_{ij}} \delta_{\sigma_i \sigma_j}} = \sum_{\{\sigma_i\}} \prod_{e_{ij}} e^{K \delta_{\sigma_i \sigma_j}}$$

where  $K = \beta J$ . The case  $q = 2$  is the Ising model, which describes (i) uniaxial magnets; (ii) structural phase transitions in binary alloys; and (iii) liquid-gas phase transitions.

Consider the limit in which the number of vertices  $n \rightarrow \infty$  on a lattice or more generally a graph  $G$ . Denote this limit for a family of graphs as  $\{G\}$  and define the reduced dimensionless free energy (per vertex) as

$$f(\{G\}) = \lim_{n \rightarrow \infty} \frac{1}{n} \ln[Z(G)]$$

The Gibbs free energy (per site) is  $-k_B T f$ . The function  $f$  encodes much information about the system; partial derivatives yield various thermodynamic functions. For example, the internal energy  $U$  and specific heat  $C$  (per site) are

$$U = -\frac{\partial f}{\partial \beta}, \quad C = k_B \beta^2 \frac{\partial^2 f}{(\partial \beta)^2}$$

The study of phase transitions is a major area in physics; a typical example is a magnetic system in which, as the temperature decreases below a critical temperature  $T_c$ , there is a nonzero uniform magnetization  $M$  (for FM case) or staggered magnetization  $M_{st}$  (for AFM case), with associated non-analytic behavior in response functions such as the specific heat and magnetic susceptibility.

Using the identity  $e^{K\delta_{\sigma_i\sigma_j}} = 1 + (e^K - 1)\delta_{\sigma_i\sigma_j} = 1 + v\delta_{\sigma_i\sigma_j}$ , where  $v = e^K - 1$ , one can write  $Z$  as

$$Z = \sum_{\{\sigma_i\}} \left[ \prod_{e_{ij}} (1 + v\delta_{\sigma_i\sigma_j}) \right]$$

Def.: Given a graph  $G = (V, E)$ , a spanning subgraph  $G' = (V, E')$  is a graph containing all of the vertices of  $G$  and a subset of the edges of  $G$ , i.e.,  $E' \subseteq E$ .

Cluster formula for  $Z$  (Fortuin-Kasteleyn rep. 1967, 1972);

$$Z(G, q, v) = \sum_{G' \subseteq G} q^{k(G')} v^{e(G')}$$

where  $k(G')$  and  $e(G')$  are the number of connected components and edges in  $G'$ . This expresses  $Z$  in a purely graph-theoretic manner without any reference to the sum over spin configurations. Without loss of generality, we take  $k(G) = 1$ .

Since  $k(G') \geq 1$  and  $e(G') \geq 0$ , the cluster representation of  $Z$  shows that  $Z(G, q, v)$  is a polynomial in  $q$  and  $v$ . Terms have  $1 \leq \deg_q \leq n(G)$  and  $0 \leq \deg_v \leq e(G)$ . Hence, one can write  $Z(G, q, v) = qZ_r(G, q, v)$ .

The cluster formula allows one to generalize  $q$  from nonnegative integers  $q = 1, 2, 3, \dots$  to nonnegative real numbers in physics. For the analysis of zeros of  $Z$  in the variables  $q$  and  $v$ , one must generalize these further to complex variables.

The proof of the cluster formula is based on the 1-1 correspondence between the terms in  $Z = \sum_{\{\sigma_i\}} \prod_{e_{ij}} (1 + v\delta_{\sigma_i\sigma_j})$  and spanning subgraphs  $G' \subseteq G$ .


Sketch of proof, using, as illustration,  $G = C_3$ , where  $C_n$  is the circuit graph with  $n$  vertices. Here

$$Z(C_3, q, v) = \sum_{\{\sigma_i\}} \prod_{e_{ij}} (1 + v\delta_{\sigma_i\sigma_j}) = \sum_{\{\sigma_i\}} (1 + v\delta_{\sigma_1\sigma_2})(1 + v\delta_{\sigma_2\sigma_3})(1 + v\delta_{\sigma_3\sigma_1})$$

There are four types of terms contributing (note relation with  $\sum_{G' \subseteq G} q^{k(G')} v^{e(G')}$ )

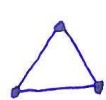
- the term 1, corresponding to the  $G'$  with three disjoint vertices, no edges, (so  $e(G') = 0$ ,  $k(G') = 3$ ), for which the sum over the  $\sigma_i$ 's yields  $q^3$ , i.e., one can choose the  $\sigma$ 's independently in  $q^3$  ways;
- $v(\delta_{\sigma_1\sigma_2} + \delta_{\sigma_2\sigma_3} + \delta_{\sigma_3\sigma_1})$ , corresponding to the three  $G'$ 's with one edge and one disjoint vertex, so  $e(G') = 1$ ,  $k(G') = 2$ . The first of these terms contributes if

example:  $G = C_3$   $G' = (V', E')$   
 $\Rightarrow 2^3 = 8$  resultant spanning subgraphs with  $V' = V$   
 with  $E' \subseteq E$  (don't confuse  $V$  and  $v$ )

  $k=3$   
 $e=0 \Rightarrow q^3$

$\left\{ \begin{array}{l} \text{---} \cdot \\ \cdot \text{---} \\ \cdot \text{---} \cdot \end{array} \right\}$   $k=2$   
 $e=1 \Rightarrow 3q^2v$

$\left\{ \begin{array}{l} \triangle \\ \nabla \\ \text{---} \cdot \end{array} \right\}$   $k=1$   
 $e=2 \Rightarrow 3qv^2$

  $k=1$   
 $e=3 \Rightarrow qv^3$

$$\Rightarrow Z(C_3, q, v) = q^3 + 3q^2v + 3qv^2 + qv^3$$

$$= (q+v)^3 + (q-1)v^3$$

This generalizes to

$$Z(C_n, q, v) = (q+v)^n + (q-1)v^n$$



$\sigma_1 = \sigma_2$ ; here one chooses  $\sigma_1 = \sigma_2$  in any of  $q$  ways, and then  $\sigma_3$  independently in any of  $q$  ways, for a total of  $q^2$  ways; similarly for the other two terms, so these terms contribute  $3q^2v$ ;

- $v^2(\delta_{\sigma_1\sigma_2}\delta_{\sigma_2\sigma_3} + \delta_{\sigma_2\sigma_3}\delta_{\sigma_3\sigma_1} + \delta_{\sigma_3\sigma_1}\delta_{\sigma_1\sigma_2})$ , corresponding to  $G'$ 's with two edges, so  $e(G') = 2$ ,  $k(G') = 1$ . For the first term to contribute, all of the  $\sigma$ 's must be equal, and there are  $q$  ways of choosing them; similarly for the other two terms, so the total contribution is then  $3qv^2$ ;
- $v^3(\delta_{\sigma_1\sigma_2}\delta_{\sigma_2\sigma_3}\delta_{\sigma_3\sigma_1})$ , corresponding to  $G' = G$ , with all edges present, so  $e(G') = 3$ ,  $k(G') = 1$ . For this term to contribute, all of the  $\sigma$ 's must be equal, amounting to  $q$  possibilities, and yielding the term  $qv^3$ .

So combining all of these terms, one gets  $Z(C_3, q, v) = q^3 + 3q^2v + 3qv^2 + qv^3$ , which is precisely  $\sum_{G' \subseteq C_3} q^{k(G')}v^{e(G')}$ .

Now  $q^3 + 3q^2v + 3qv^2 + qv^3 = (q + v)^3 + (q - 1)v^3$ , so  
 $Z(C_3, q, v) = (q + v)^3 + (q - 1)v^3$

By the same methods, one obtains the generalization

$$Z(C_n, q, v) = (q + v)^n + (q - 1)v^n$$

One can also consider the Potts model in an external magnetic field  $H$  that favors or disfavors spin values in a subset  $I_s = \{1, \dots, s\}$  of the total set of  $q$  possible spin values. Define  $h = \beta H$  and  $w = e^h$ . Given a spanning subgraph  $G' \subseteq G$  with  $k(G')$  connected components, denote these as  $G'_i$ ,  $i = 1, \dots, k(G')$ .

We have obtained the generalized partition function for this case:

$$Z(G, q, s, v, w) = \sum_{G' \subseteq G} v^{e(G')} \prod_{i=1}^{k(G')} (q - s + sw^{n(G'_i)})$$

(Chang and RS, J. Phys. A42, 385004 (2009); J. Stat. Phys. 138, 496 (2010); RS and Xu, J. Stat. Phys. 139, 27 (2010)).

The factor  $q - s + sw^m$  for each connected component  $G'_i \in G'$  can be understood since each of the spins must have the same value  $\sigma$  in this term in the cluster sum; for the  $s$  cases where  $\sigma \in I_s$ , this gives  $sw^{n(G'_i)}$ , while for the  $q - s$  cases where  $\sigma \notin I_s$ , this gives  $q - s$ .

Henceforth, we take  $H = 0$ , i.e., zero external magnetic field.

Next, we define two important graph-theoretic polynomials:

Def. The chromatic polynomial  $P(G, q)$  is the number of ways of assigning  $q$  colors to the vertices of  $G$  such that no two adjacent vertices have the same color. This is called a proper  $q$ -coloring of (the vertices of)  $G$ , and so  $P(G, q)$  is the number of proper  $q$ -colorings of  $G$ . The minimum number of colors needed for a proper  $q$ -coloring of  $G$  is the chromatic number,  $\chi(G)$ .

In the antiferromagnetic Potts model, consider the limit  $T \rightarrow 0$ , so  $K \rightarrow -\infty$  (since  $K = \beta J$  and  $J < 0$ ) and  $v = e^K - 1 \rightarrow -1$ . In this limit, the only spin configurations that contribute to  $Z(G, q, v = -1)$  are those for which adjacent spins have different values. Hence, the  $T = 0$  limit of the Potts antiferromagnet partition function is the chromatic polynomial:

$$Z(G, q, -1) = P(G, q)$$

$P(G, q)$  always contains a factor  $q$ , so can write  $P(G, q) = qP_r(G, q)$ .

Def. A loop in a graph is an edge that connects a vertex back to itself, so the vertex is adjacent to itself. Since a proper  $q$ -coloring of  $G$  requires adjacent vertices to have different colors,  $P(G, q) = 0$  if  $G$  contains a loop.

Graph coloring has long been of interest in mathematical graph theory; early work by Birkhoff (1912, 1930) and Whitney (1932), subsequent work by Tutte, Read, and many others. One aspect of this dealt with map coloring, i.e., face-coloring of planar graphs.

Def. a proper  $q$ -coloring of the faces of a graph is an assignment of colors, from a set of  $q$  colors, to the faces of a graph such that no two adjacent faces (faces that share an edge) have the same color.

For a planar graph  $G$ , there is a 1-1 correspondence between the vertices of  $G$  and the faces of the planar dual graph  $G^*$ . Therefore,  $P(G, q)$  equivalently counts the proper  $q$ -colorings of the vertices of  $G$  and the proper  $q$ -colorings of the faces of  $G^*$ .

Def. An edge in  $G^*$  which, if cut, would increase the number of components of  $G^*$  by 1 is called a bridge. A bridge in  $G^*$  leads to a face being adjacent to itself across the bridge. Since adjacent faces must have different colors in a proper  $q$ -coloring of the faces of a planar graph  $G^*$ , this is not possible if  $G^*$  contains any bridges. N.B.: A bridge in  $G^*$  is dual to a loop in  $G$ .

The Four-Color Theorem: If  $G$  is a planar graph with no loops, i.e.,  $G^*$  is a planar graph with no bridges, then  $P(G, 4) > 0$ , i.e., there exists a proper  $q$ -coloring of the vertices of  $G$  with  $q = 4$  colors, or equivalently, there exists a proper  $q$ -coloring of the faces of  $G^*$  with  $q = 4$  colors. This was proved in 1976 by Appel and Haken.

The chromatic polynomial is of interest not just in graph theory but also in applied mathematics and engineering. One application is the following frequency allocation problem:

Consider  $n$  radio broadcast transmitter stations; let each of these be represented by a vertex of a graph  $G$  and define two transmitters as being adjacent (joined by a edge) if they are closer than a certain distance to each other.

Now assign frequencies from a set of  $q$  values to these transmitters, subject to the condition that adjacent stations should use different frequencies to avoid interference. The number of ways of doing this is  $P(G, q)$ .

A graph polynomial of major importance in mathematical graph theory is the Tutte (also called Tutte-Whitney) polynomial,  $T(G, x, y)$  (Tutte, 1947, 1953, 1967)

$$T(G, x, y) = \sum_{G' \subseteq G} (x - 1)^{k(G') - k(G)} (y - 1)^{c(G')}$$

where  $G'$  is a spanning subgraph of  $G$  and  $k(G')$  and  $c(G')$  denote the number of components and (linearly independent) cycles in  $G'$ , respectively.

Since  $k(G') - k(G) \geq 0$  and  $c(G') \geq 0$ , it follows that  $T(G, x, y)$  is a polynomial in  $x$  and  $y$ ; terms have  $0 \leq \deg_x \leq n - 1$  and  $0 \leq \deg_y \leq c(G)$

The Potts model partition function  $Z(G, q, v)$  is equivalent to the Tutte polynomial  $T(G, x, y)$  with the identification

$$x = 1 + \frac{q}{v}, \quad y = v + 1$$

so  $q = (x - 1)(y - 1)$  and  $x - 1 = q/v$ . Note that  $c(G') = e(G') + k(G') - n(G')$  and hence, since  $n(G') = n(G)$ ,  $c(G') = e(G') + k(G') - n(G)$ .

Showing this equivalence of  $Z(G, q, v)$  and  $T(G, x, y)$ :

$$\begin{aligned} T(G, x, y) &= (x - 1)^{-k(G)} (y - 1)^{-n(G)} \sum_{G' \subseteq G} (x - 1)^{k(G')} (y - 1)^{e(G') + k(G')} \\ &= (x - 1)^{-k(G)} (y - 1)^{-n(G)} \sum_{G' \subseteq G} \left( \frac{q}{v} \right)^{k(G')} v^{e(G') + k(G')} \\ &= (x - 1)^{-k(G)} (y - 1)^{-n(G)} \sum_{G' \subseteq G} q^{k(G')} v^{e(G')} \\ &= (x - 1)^{-k(G)} (y - 1)^{-n(G)} Z(G, q, v) , \end{aligned}$$

i.e.,

$$T(G, x, y) = (q/v)^{-k(G)} v^{-n(G)} Z(G, q, v)$$

As an example, from this relation, for the circuit graph  $C_n$ , using  $q = (x - 1)(y - 1)$ , so  $(x - 1) = q/v$ , we have

$$\begin{aligned} Z(C_n, q, v) &= (q + v)^n + (q - 1)v^n = v^n \left[ \left(1 + \frac{q}{v}\right)^n + (xy - x - y) \right] \\ &= v^n \left[ x^n - x + y(x - 1) \right] \end{aligned}$$

so

$$\begin{aligned} T(C_n, x, y) &= v^{-n} (q/v)^{-1} Z(C_n, q, v) = \frac{x^n - x + y(x - 1)}{q/v} \\ &= \frac{x^n - x}{x - 1} + y = \left( \sum_{j=1}^{n-1} x^j \right) + y \end{aligned}$$

so  $T(C_1, x, y) = y$ ,  $T(C_2, x, y) = x + y$ , etc.

Although the calculation of  $Z(C_n, q, v)$  (equivalently,  $T(C_n, x, y)$ ) is easy, for a general graph  $G$  and for arbitrary values of  $q$  and  $v$ , the calculation of the Potts/Tutte polynomial takes a time that grows exponentially with  $n$ , as is obvious from the original expression for  $Z$  as a sum over all spin configurations, of which there are  $q^n = e^{n \ln q}$ .



Special cases of the Tutte polynomial yield many graph-theoretic functions of interest. One of these is the chromatic polynomial; for  $v = -1$ , i.e.,  $y = 0$ , since  $Z(G, q, v = -1) = P(G, q)$ , one has

$$P(G, q) = (-q)^{k(G)} (-1)^{n(G)} T(G, x = 1 - q, y = 0)$$

In a series of papers since the 1990s we have obtained exact calculations of  $Z(G, q, v)$  and  $P(G, q)$  on various families of graphs (mainly lattice strips) and have analyzed quantities such as  $f(\{G\}, q, v)$  in the limit as  $n \rightarrow \infty$  (see refs. at end).

Special valuations of  $T(G, x, y)$  count various types of subgraphs of  $G$ .

Def. A connected graph that does not contain any cycles (circuits) is a tree graph.

Def. Given a graph  $G$ , a spanning subgraph  $G' \subseteq G$  that is a tree graph is a spanning tree (ST). Denote the number of spanning trees in  $G$  as  $N_{ST}(G)$ .

Setting  $x = 1$  in  $T(G, x, y)$  restricts the  $G'$ s that contribute to those that are connected, i.e.,  $k(G') = k(G) = 1$ . Setting  $y = 1$  restricts the  $G'$ s that contribute to those having no cycles, so that  $c(G') = 0$ .

Hence, setting  $x = y = 1$  picks out  $G'$ 's that are spanning subgraphs with  $c(G') = 0$ , i.e., spanning trees. So

$$T(G, 1, 1) = N_{ST}(G)$$

Def. Given a graph  $G$ , a spanning subgraph  $G' \subseteq G$  that has no cycles but may be disconnected, i.e., consist of more than one component, is called a spanning forest (SF) of  $G$ . Denote the number of spanning forests in  $G$  as  $N_{SF}(G)$ .

One can relax the restriction on connectedness by setting  $x = 2$ , so that  $(x - 1)^{k(G') - k(G)} = 1$ , independent of  $k(G')$ . Thus,

$$T(G, 2, 1) = N_{SF}(G)$$

One can keep the restriction on connectedness but include  $G'$ 's with cycles by setting  $y = 2$ ; then  $(y - 1)^{c(G')} = 1$  independent of  $c(G')$ . Hence

$$T(G, 1, 2) = N_{CSSG}(G)$$

where  $N_{CSSG}$  is the number of connected spanning subgraphs of  $G$ .

If one sets  $x = y = 2$ , then the summand is just 1, so this counts all of the spanning subgraphs of  $G$ . These are enumerated by either including or excluding an edge between each pair of adjacent vertices, which is a 2-fold choice for each edge, so

$$T(G, 2, 2) = 2^{e(G)}$$

Def. The degree  $\Delta$  of a vertex in a graph is the number of edges that connect to it. A graph whose vertices all have the same degree  $\Delta$  is termed a  $\Delta$ -regular graph.

Def. An Archimedean lattice is a  $\Delta$ -regular tiling of the plane with one or more types of regular polygons, such that all vertices are equivalent.

A particular Archimedean lattice  $\Lambda$  may be defined by the ordered sequence of regular polygons that one traverses in a circuit around any vertex:

$$\Lambda = \left( \prod_i p_i^{a_i} \right),$$

where the  $i$ 'th polygon has  $p_i$  sides and appears  $a_i$  times contiguously in the sequence (it can also occur non-contiguously).

Thus, e.g., the honeycomb (hc), square (sq), and triangular (tri) lattices are denoted as  $6^3$ ,  $4^4$ , and  $3^6$ .

For a wide variety of families of  $n$ -vertex graphs, including strips of regular lattices, as  $n \rightarrow \infty$ ,  $N_{ST}(G)$ ,  $N_{SF}(G)$ , and  $N_{CSSG}(G)$  (as well as  $N_{SSG}(G)$ ) grow exponentially with  $n$ .

Hence, it is of interest to study the exponential growth constants

$$\phi(\{G\}) = \lim_{n(G) \rightarrow \infty} [N_{SF}(G)]^{1/n(G)}, \quad \sigma(\{G\}) = \lim_{n(G) \rightarrow \infty} [N_{CSSG}(G)]^{1/n(G)}$$

Using our solutions for  $T(G, x, y)$  on strips of various lattices, we have obtained quite accurate determinations of  $\phi(\Lambda)$  and  $\sigma(\Lambda)$  for several Archimedean lattices. (Chang and RS, Int. J. Mod. Phys. B 34, 2050249 (2020) [arXiv:2002.07150]; Int. J. Mod. Phys. B 35, 2150085 (2021) [arXiv:2012.13468]). Note the monotonic growth of  $\phi$  and  $\sigma$  with  $\Delta$ .

$\Lambda$	$\Delta(\Lambda)$	$\phi(\Lambda)$	$\sigma(\Lambda)$
$(4 \cdot 8^2)$	3	$2.77931 \pm 0.00018$	$2.3195 \pm 0.017$
$(6^3) = \text{hc}$	3	$2.80428 \pm 0.00050$	$2.333 \pm 0.011$
$(4^4) = \text{sq}$	4	$3.687 \pm 0.012$	$3.687 \pm 0.012$
$(3 \cdot 6 \cdot 3 \cdot 6)$	4	$3.602 \pm 0.012$	$3.74 \pm 0.10$
$(3^3 \cdot 4^2)$	5	$4.530 \pm 0.024$	$5.486 \pm 0.041$
$(3^2 \cdot 4 \cdot 3 \cdot 4)$	5	$4.503 \pm 0.065$	$5.465 \pm 0.058$
$(3^6) = \text{tri}$	6	$5.444 \pm 0.051$	$7.864 \pm 0.0028$

# Chromatic Polynomials and Ground State Entropy of Potts Antiferromagnet

A quantity of particular interest is the ground state degeneracy, per site, of the Potts antiferromagnet,

$$W(\{G\}, q) = \lim_{n \rightarrow \infty} P(G, q)^{1/n}$$

The associated ground state entropy per site is  $S_0(\{G\}, q) = k_B \ln[W(\{G\}, q)]$ .

The  $q$ -state Potts antiferromagnet at  $T = 0$  is noteworthy as a system that, for a given type of graph  $G$  and sufficiently large  $q$ , exhibits nonzero ground state entropy (per site)  $S_0$ , or equivalently,  $W > 1$ .

There are physical systems that exhibit this type of residual low-temperature entropy, such as water ice, for which  $W = 1.51$ , i.e., the entropy per molecule is  $S_0/k_B = \ln W = 0.41$  (studied by Linus Pauling).

This is due to the fact that ice is a hydrogen-bonded molecular crystal and there is a twofold possibility for the H atom in each hydrogen bond, to be closer to one oxygen atom or the other. Even with the constraint of local electric neutrality, this produces exponentially many ground state configurations of equal (minimal) energy, and hence a finite ground state entropy of ice.

Def. A graph  $G$  is bipartite if  $G = G_e \oplus G_o$ , such that for each vertex in the even (e) subgraph  $G_e$ , all of the adjacent vertices are in the odd subgraph  $G_o$  and vice versa.

Simple proof of  $S_0 > 0$  for the Potts antiferromagnet on a bipartite graph  $G_{bp}$ . for  $q > 2$ . This proof uses a lower bound on  $P(G, q)$ .

This lower bound is proved as follows. Assign one color to all of the vertices on  $G_e$ , which can be done in any of  $q$  ways. Then independently for each vertex on  $G_o$ , one can choose the color in any of  $q - 1$  ways. Therefore,

$$P(G_{bp}, q) \geq q(q - 1)^{n/2}$$

Hence, for  $n \rightarrow \infty$ , one has  $W(\{G\}, q) \geq \sqrt{q - 1}$  and  $S_0 \geq (k_B/2) \ln(q - 1)$ .

So for  $q > 2$ , there is nonzero ground state entropy per site.

We have obtained stronger lower bounds on  $W(\{G\}, q)$  and  $S_0(\{G\}, q)$  for a large variety of two-dimensional lattices (RS and Tsai, Phys. Rev. E 55, 6791 (1997); Phys. Rev. E 56, 2733 (1997); Phys. Rev. E 56, 4111 (1997); Chang and RS, Phys. Rev. E 91, 052142 (2015)).

# Zeros of Chromatic and Potts/Tutte Polynomials and their Accumulation Sets as $n \rightarrow \infty$

Since  $Z(G, q, v)$  is a polynomial in  $q$  and  $v$ , it is of interest to analyze its zeros.

We have analyzed the zeros of  $Z(G, q, v)$  in the complex  $q$  plane for fixed  $v$ , and in the complex  $v$  plane for fixed  $q$  for many families of graphs including lattice strips and necklace graphs.

We study the behavior of these zeros of  $Z(G, q, v)$  for  $G$  a lattice strip graph in the limit of infinite length with fixed width, whence  $n \rightarrow \infty$ ; similarly with necklace graphs with infinite circuit length. In this limit, zeros accumulate to form certain curves and possible line segments, generically denoted as the loci  $\mathcal{B}_q$  for fixed  $v$  and  $\mathcal{B}_v$  for fixed  $q$ .

For a lattice strip of fixed width  $L_y$  and arbitrarily great length  $L_x = m$ , we obtain  $Z(G, q, v) = \sum_j c_j(q) (\lambda_j)^m$ , where  $\lambda_j$  are certain functions of  $q$  and  $v$ , and  $c_j(q)$  are certain coefficients. For generic  $q$ , the limit  $m \rightarrow \infty$  is dominated by the  $\lambda_j$  of maximal magnitude.

Zeros occur where there is a degeneracy of two or more dominant  $\lambda$ 's, making cancellations possible. The condition that two dominant  $\lambda$ 's are equal in magnitude

defines algebraic curves (and possible lines). These are the loci  $\mathcal{B}_q$  for fixed  $v$  and  $\mathcal{B}_v$  for fixed  $q$  for these lattice strips. Early studies of  $\mathcal{B}_q$  for  $v = -1$  by Biggs; Read; Beraha, Kahane, and Weiss.

The number of  $\lambda$ 's depends on  $L_y$  and the longitudinal and transverse boundary conditions (BC). For example, for  $Z(G, q, v)$  on cyclic strips,  $N_{Z, L_y, \lambda} = \binom{2L_y}{L_y}$ , so  $N_\lambda = 2, 6, 20, 70$  for  $L_y = 1, 2, 3, 4$ . A subset of these remain for  $P(G, q) = Z(G, q, -1)$ :  $N_{P, L_y, \lambda} = 2, 4, 10, 26$  for  $L_y = 1, 2, 3, 4$ . These numbers increase rapidly as  $L_y$  increases. Nevertheless, we were able to carry out exact calculations of  $Z$  and  $P$  for a variety of lattice types (square, triangular, honeycomb..) and widths of strips with arbitrarily great lengths.

The  $\lambda$ 's are roots of algebraic equations with coefficients that are polynomials in  $q$  and  $v$ . Although we cannot solve for these in terms of radicals when the degrees of the algebraic equations are  $\geq 5$ , the combinations of the  $\lambda_j^m$  powers that occur in  $Z(G, q, v)$  and  $P(G, q)$  are symmetric functions of the roots and hence one can express them (using Newton's identities) in terms of the polynomial coefficients in these equations.



example: cyclic strip of square lattice with width  $L_y = 2$  (RS, Physica A 283, 388 (2000)),  $N_{Z,\lambda} = 6$ :

$$Z([sq, 2 \times m, cyc], q, v) = (\lambda_{2,0,1}^m + \lambda_{2,0,2}^m) + (q-1)(\lambda_{2,1,1}^m + \lambda_{2,1,1}^m + \lambda_{2,1,1}^m) + (q^2 - 3q + 1)\lambda_{2,2,1}^m$$

where

$$\lambda_{2,0,(1,2)} = \frac{1}{2} \left[ v^3 + 4v^2 + 3qv + q^2 \pm \left( v^6 + 4v^5 - 2qv^4 - 2q^2v^3 + 12v^4 + 16qv^3 + 13q^2v^2 + 6q^3v + q^4 \right)^{1/2} \right]$$

$$\lambda_{2,1,1} = v(q + v), \quad \lambda_{2,1,1} = v^2,$$

$$\lambda_{2,1,(2,3)} = \frac{v}{2} \left[ q + v(v + 4) \pm \left( v^4 + 4v^3 + 12v^2 - 2qv^2 + 4qv + q^2 \right)^{1/2} \right]$$

For the chromatic polynomial special case  $v = -1$ ,  $N_{P,\lambda} = 4$ :

$$P([sq, 2 \times m, cyc], q) = \lambda_{2,0,1}^m + (q-1)(\lambda_{2,1,1}^m + \lambda_{2,1,2}^m) + (q^2 - 3q + 1)\lambda_{2,2,1}^m$$

where

$$\lambda_{2,0,1} = q^2 - 3q + 3, \quad \lambda_{2,1,1} = 1 - q, \quad \lambda_{2,1,2} = 3 - q, \quad \lambda_{2,2,1} = 1$$

Early study of zeros in  $v$  for the special case of the  $q = 2$  Potts (= Ising) model on the square lattice by Fisher (1965). Zeros in  $q$  for the case  $v = -1$  where  $Z(G, q, -1) = P(G, q)$  are called chromatic zeros.

As one crosses a boundary on  $\mathcal{B}_q$  or  $\mathcal{B}_v$ , the dominant  $\lambda$ , and hence the resultant  $f$  and/or  $W$  function changes non-analytically.

We have calculated  $\mathcal{B}_q$  and  $\mathcal{B}_v$  for the  $n \rightarrow \infty$  limits of many families of graphs, typically infinite-length strips of regular lattices. The study of these boundaries ties together graph theory, complex analysis, and algebraic geometry, and also relates these to statistical physics.

For a long but finite-length strip, many zeros lie close to the asymptotic locus  $\mathcal{B}_q$  or locus  $\mathcal{B}_v$  on which they merge as  $n \rightarrow \infty$ .

If one includes an external magnetic field, then one can also calculate zeros of  $Z(G, q, s, v, w)$  in  $w = e^h$ . Pioneering study of these by Lee and Yang for the Ising case  $q = 2$  (1952). We have also studied these zeros for general  $q$  and  $s$  but restrict our discussion here to the case of zero external magnetic field.

Illustrative calculation of  $\mathcal{B}_v$  and  $\mathcal{B}_q$  for a given limit  $\{G\}$ . Let us consider the family of circuit graphs  $C_n$ . Recall that

$Z(C_n, q, v) = (q + v)^n + (q - 1)v^n = \lambda_{C,0}^n + (q - 1)\lambda_{C,1}^n$ , where  $\lambda_{C,0} = q + v$  and  $\lambda_{C,1} = v$ . In the  $n \rightarrow \infty$  limit, denoted  $\{C\}$ , one or the other of these  $\lambda$ 's will generically have a larger magnitude than the other and hence will dominate the limit, so that the reduced free energy

$$f = f(\{C\}, q, v) = \lim_{n \rightarrow \infty} \frac{1}{n} \ln Z(C_n, q, v)$$

is  $f = \ln(q + v)$  in the region  $|q + v| > |v|$  and the different form  $f = \ln v$  in the region  $|v| > |q + v|$ . On the boundary curve separating these two regions,  $f$  changes form nonanalytically.

This boundary locus is given by the condition of equality in magnitude of the two  $\lambda$ 's, namely  $|q + v| = |v|$ . Since zeros of  $Z(C_n, q, v)$  occur where the two (dominant)  $\lambda$ 's are equal in magnitude, enabling cancellation, this is also the continuous accumulation set of zeros of  $Z(C_n, q, v)$  as  $n \rightarrow \infty$ .

In the complex  $v$  plane, the locus  $\mathcal{B}_v$  of solutions to the equation  $|q + v| = |v|$  is the infinite vertical line  $v = -(q/2) + ir$ ,  $-\infty < r < \infty$ , which crosses the real- $v$  axis at  $v = -q/2$ .

The solution to  $|q + v| = |v|$  in the complex  $q$  plane,  $\mathcal{B}_q$ , is the circle centered at  $q = -v$  with radius  $|v|$ . This crosses the real  $q$  axis at  $q = -2v$  and  $q = 0$ . In

particular, for the chromatic polynomial, for which  $v = -1$ , this is the circle  $|q - 1| = 1$  centered at  $q = 1$ , passing through  $q = 0$  and  $q = 2$ .

We denote the maximal point where  $\mathcal{B}_q$  intersects the real  $q$  axis for a given  $v$  as  $q_c(v)$  and simply  $q_c$  for the chromatic zeros, where  $v = -1$ . Thus,  $q_c = 2$  for this family of graphs.

Hence, in the chromatic polynomial case, the boundary  $\mathcal{B}_q$  separates the complex  $q$  plane into two regions, namely the exterior and interior of the circle  $|q - 1| = 1$  (see figure). Outside,  $W = q - 1$ ; inside,  $|W| = 1$ .

For the (infinite-length) cyclic strip of the square lattice with width  $L_y = 2$ ,  $\mathcal{B}_q$  separates the  $q$  plane into four regions (see fig.): (i) in exterior,  $W = \sqrt{q^2 - 3q + 3}$ ; (ii) in innermost region,  $W = 3 - q$ ; (iii) in the two complex-conjugate bubble regions,  $W = q - 1$ .

Similar but more complicated loci  $\mathcal{B}_q$  for infinite-length strips of larger widths and other lattices (see refs. at end).

A general method for calculating  $Z(G, q, v)$  for any graph  $G$  is the following. Let  $G - e$  denote the graph  $G$  with the edge  $e$  deleted and let  $G/e$  denote the graph  $G$  with the edge  $e$  deleted and the two vertices which it connected identified, i.e.,  $G$  contracted on the edge  $e$ .  $Z(G, q, v)$  satisfies the deletion-contraction relation (DCR)

$$Z(G, q, v) = Z(G - e, q, v) + vZ(G/e, q, v)$$

This can be seen from the Hamiltonian representation of  $Z(G, q, v)$  and is equivalent to the identity (for  $e = e_{ij}$ )  $\exp(K\delta_{\sigma_i\sigma_j}) = 1 + v\delta_{\sigma_i\sigma_j}$ ; there are two possibilities: the two  $\sigma$ 's on the vertices joined by the edge  $e$  are:

- different, in which case  $Z$  is the same as if this edge were removed, corresponding to the 1; or
- the  $\sigma$ 's are the same, which is accounted for by the  $v\delta_{\sigma_i\sigma_j}$  term in the above identity.

We use an iterative application of the DCR and related techniques for our calculations of  $Z(G, q, v)$  on lattice strips of given widths  $L_y$  and arbitrarily great lengths  $L_x$ . Lattice types include square, triangular, honeycomb, kagomé, etc.

Types of boundary conditions (BC) for lattice strips are denoted F = free, P = periodic, T = twisted. The  $n \rightarrow \infty$  limit is obtained by taking the strip length  $L_x \rightarrow \infty$ .

- free:  $FBC_x, FBC_y$
- cyclic:  $PBC_x, FBC_y$
- Möbius:  $TPBC_x, FBC_y$
- cylindrical:  $FBC_x, PBC_y$
- toroidal:  $PBC_x, PBC_y$
- Klein-bottle:  $TPBC_x, PBC_y$
- $G_D$  - self-dual BC for square lattice strips

We mainly focus here on the loci  $\mathcal{B}_q$  obtained in the infinite-length limit of the strips. This depends on both the type of lattice and on the boundary conditions in the transverse and longitudinal directions. We (with Matveev, Tsai, Chang) have calculated these for square, triangular, honeycomb, and other lattice strips (also work with/by Brown, Jacobsen, Salas, Sokal); We then discuss work on  $\mathcal{B}_q$  with Chang and Roeder.

One can also analyze the locus  $\mathcal{B}_v$ , which separates different regions of the  $v$  plane. On a 2D lattice, these are complex- $v$  extensions of physical phases of the  $q$ -state Potts model (PM, FM, possible AFM).

We have found several general properties of  $\mathcal{B}_q$  from these calculations of  $\mathcal{B}_q$  for infinite-length lattice strips. For example, for cyclic (PBC<sub>*x*</sub>, FBC<sub>*y*</sub>) and Möbius (TPCB<sub>*x*</sub>, FBC<sub>*y*</sub>) strips, general properties include:

- $\mathcal{B}_q$  separate the  $q$  plane into different regions
- The left-most point where  $\mathcal{B}_q$  intersects (crosses) the real  $q$  axis is at  $q = 0$ .
- For strips of the square lattice, the right-most point where  $\mathcal{B}_q$  crosses the real axis is  $q_c = 2$  for  $L_y = 1, 2$  and increases as the strip width  $L_y$  increases, taking the values  $q_c = 2.34, 2.49, 2.58$  for  $L_y = 3, 4, 5$ . We conjecture that for cyclic strips with  $L_y \geq 2$ , (i)  $q_c$  is a monotonically increasing function of strip width  $L_y$  and (ii)  $\lim_{L_y \rightarrow \infty} q_c = 3$ , which would agree with the property that the  $q = 3$  Potts AFM on the (infinite) square lattice has a  $T = 0$  critical point (at  $v = -1$ ).
- For strips of the triangular lattice,  $q_c$  is a nondecreasing function of  $L_y$ , and we conjecture that  $\lim_{L_y \rightarrow \infty} q_c = 4$ , which would agree with the property that the  $q = 4$  Potts AFM on the (infinite) triangular lattice has a  $T = 0$  critical point.
- These connections with  $T = 0$  critical points of Potts AFM show interesting link between singularities in  $q$  plane for fixed  $v$  and in  $v$  plane for fixed  $q$  - different slices of an algebraic variety in  $\mathbb{C}^2$  space of  $(q, v)$ .

For self-dual strips of the square lattice with periodic longitudinal BC,

- $\mathcal{B}_q$  again separates the  $q$  plane into regions, but
- the left-most point where  $\mathcal{B}_q$  crosses the real  $q$  axis is at  $q = 1$  instead of  $q = 0$ .
- $q_c = 3$  for all  $L_y$  - this is understandable since these graphs maintain the same self-duality property as the two-dimensional square lattice, whereas, in contrast, the cyclic square-lattice strips are not self-dual.

We find that  $q_c$  does not increase monotonically as a function of width  $L_y$  for torus and Klein-bottle strips.

For most strips with free or cylindrical boundary conditions,  $\mathcal{B}_q$  consists of self-conjugate arcs, complex-conjugate pairs of arcs and possible real line segments that do not separate the  $q$  plane into different regions.

Some illustrative figures for regular lattice strips follow. For others, see refs. at end.



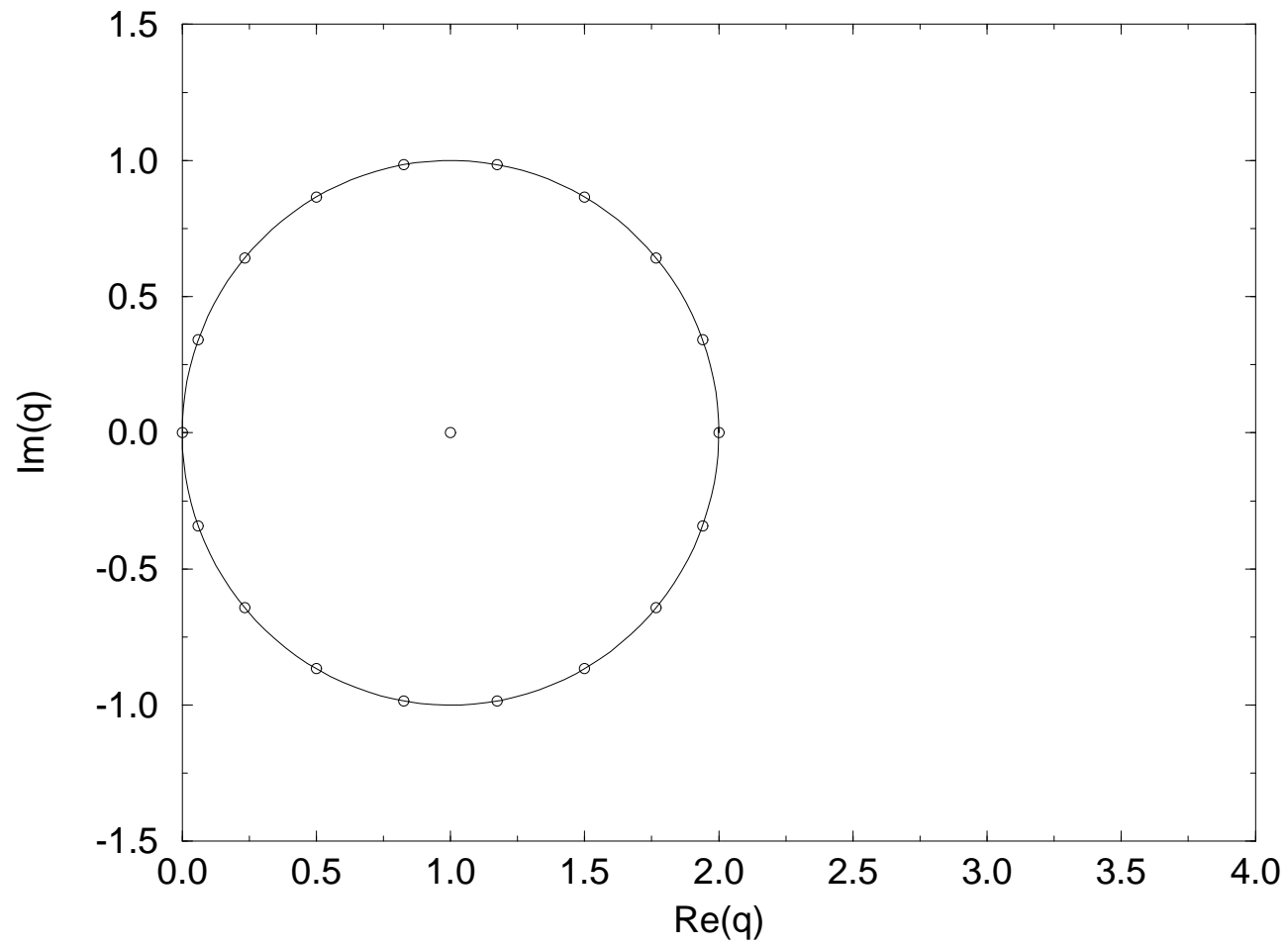


Figure 1: Locus  $\mathcal{B}_q$  in the  $q$  plane for the  $n \rightarrow \infty$  limit of the circuit graph  $C_n$ . Chromatic zeros for  $B_n$  with  $n = 19$  are shown for comparison. From R. Shrock and S.-H. Tsai, Phys. Rev. E55, 5165 (1997).

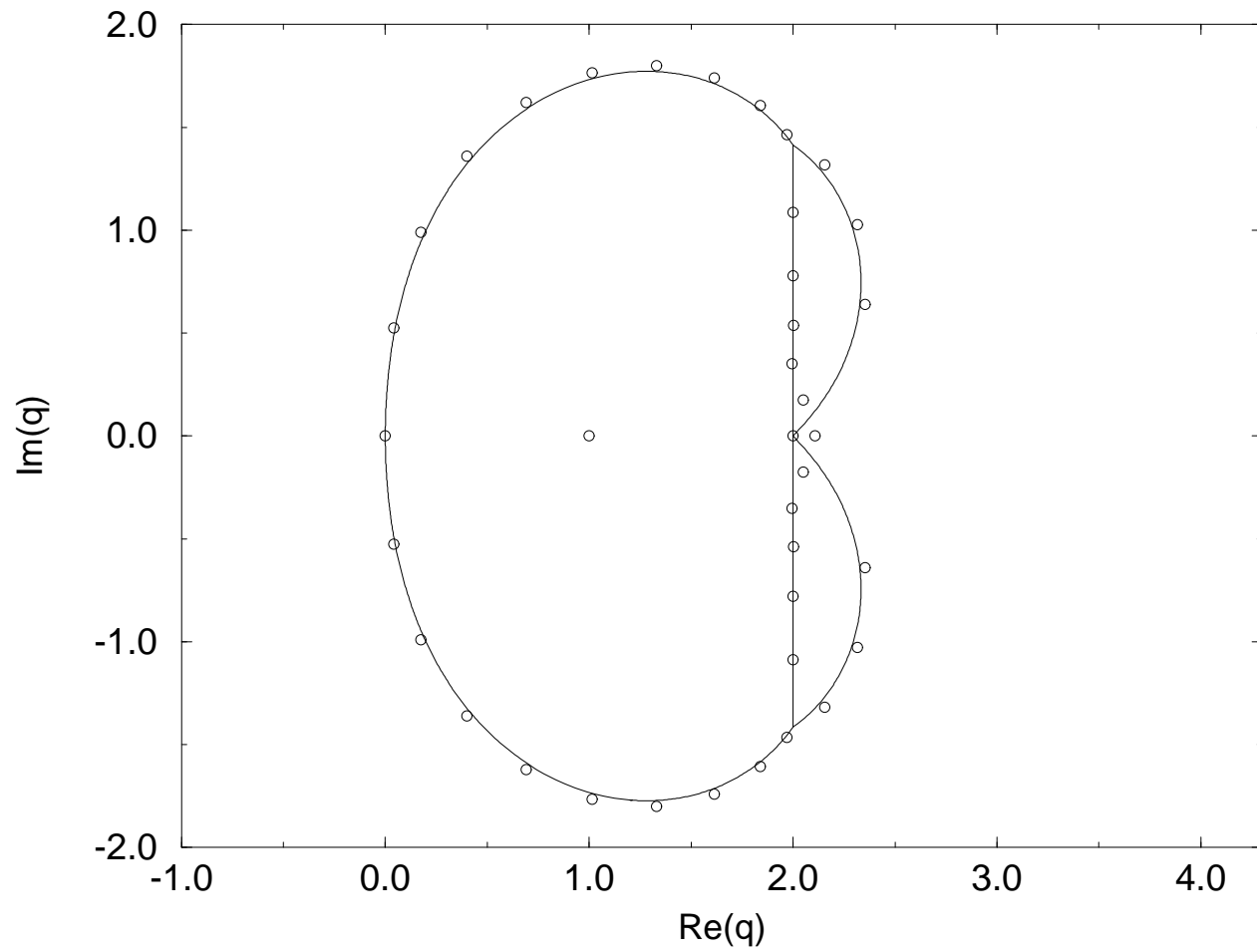


Figure 2: Locus  $\mathcal{B}_q$  in the  $q$  plane for the  $L_x \rightarrow \infty$  limit of the cyclic or Möbius strip of the square lattice with width  $L_y = 2$ . Chromatic zeros for the cyclic strip with  $L_x = 19$  and thus  $n = 38$  vertices are shown for comparison. From R. Shrock and S.-H. Tsai, Phys. Rev. E55, 5165 (1997).

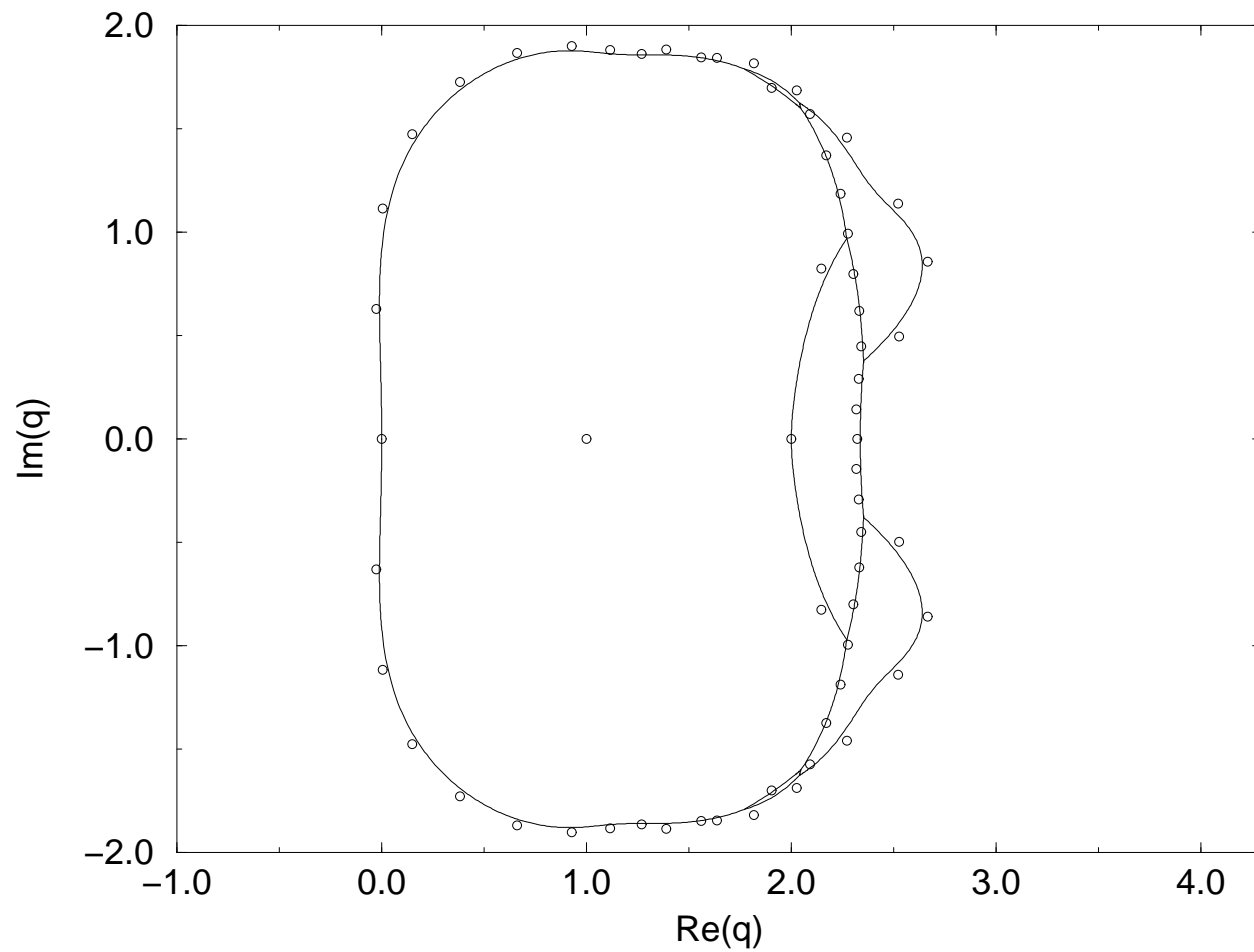


Figure 3: Locus  $\mathcal{B}_q$  for the  $L_x \rightarrow \infty$  limit of the cyclic or Möbius strip of the square lattice with width  $L_y = 3$ . Chromatic zeros for the cyclic strip with  $L_x = 20$  and thus  $n = 60$  vertices are shown for comparison. From R. Shrock and S.-H. Tsai, Phys. Rev. E60, 3512 (1999).

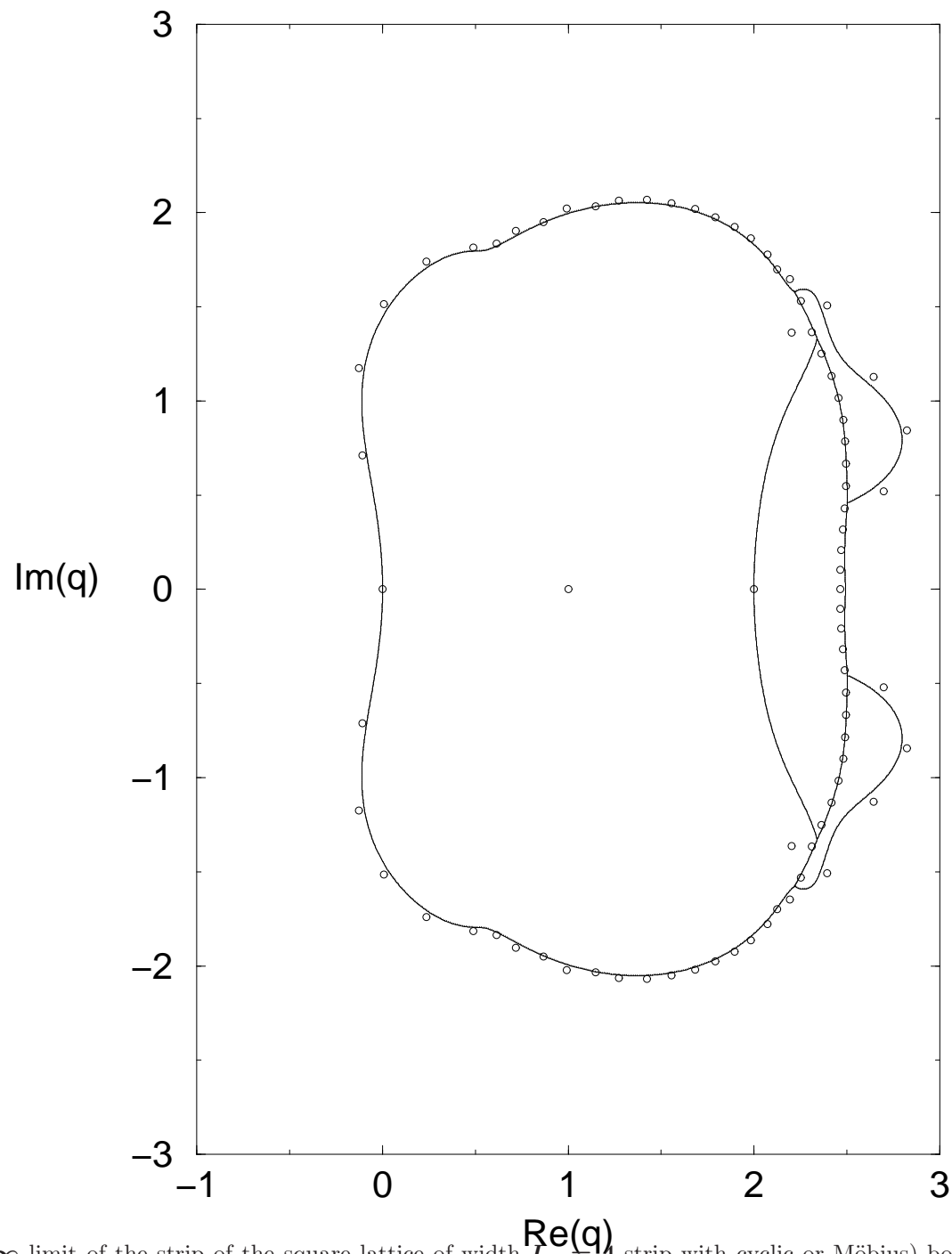


Figure 4: Locus  $\mathcal{B}_q$  for the  $L_x \rightarrow \infty$  limit of the strip of the square lattice of width  $L_y = 4$  strip with cyclic or Möbius) boundary conditions. For comparison, chromatic zeros calculated for the cyclic strip with  $L_x = 20$  and thus  $n = 80$  vertices are shown. From S.-C. Chang and R. Shrock, Physics A290, 402 (2001), Physica A316, 335 (2002).

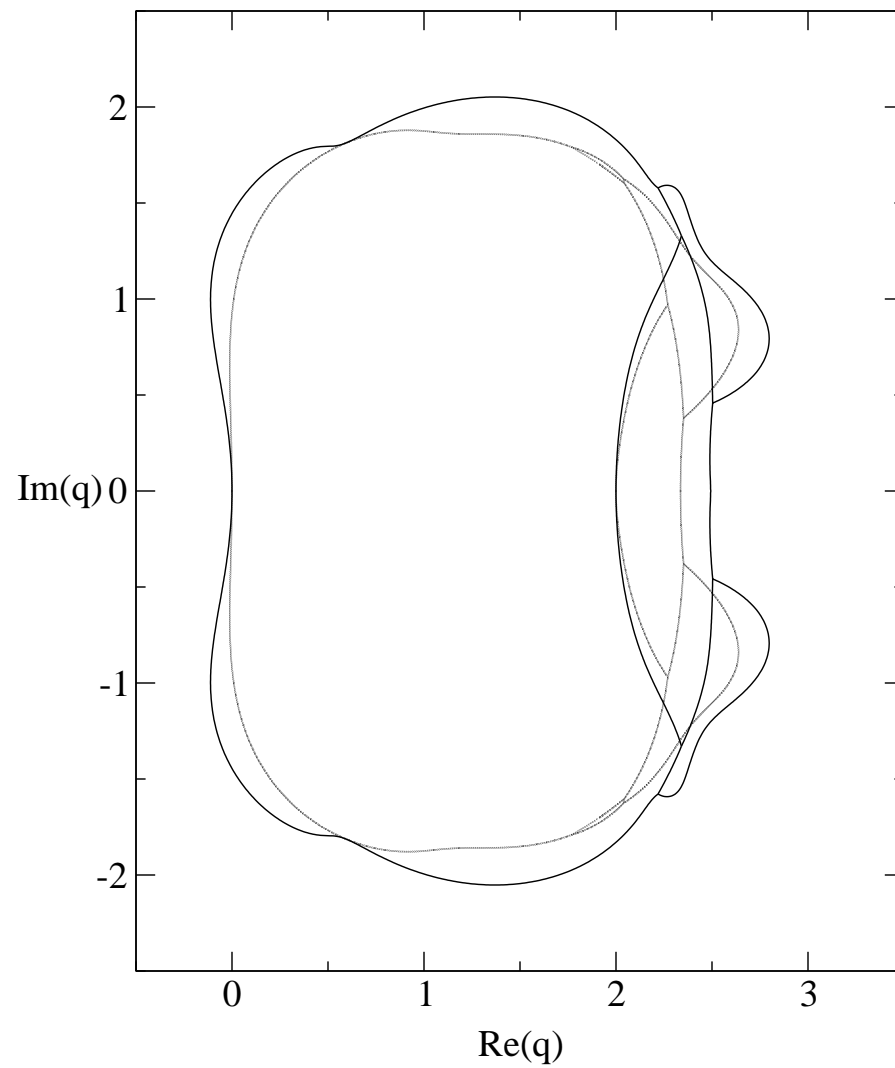


Figure 5: Comparison of loci  $\mathcal{B}_q$  for the  $L_x \rightarrow \infty$  limits of the strip of the square lattice with cyclic or Möbius boundary conditions with widths  $L_y = 3$  and  $L_y = 4$ . From S.-C. Chang and R. Shrock, *Physica A*292, 307 (2001).

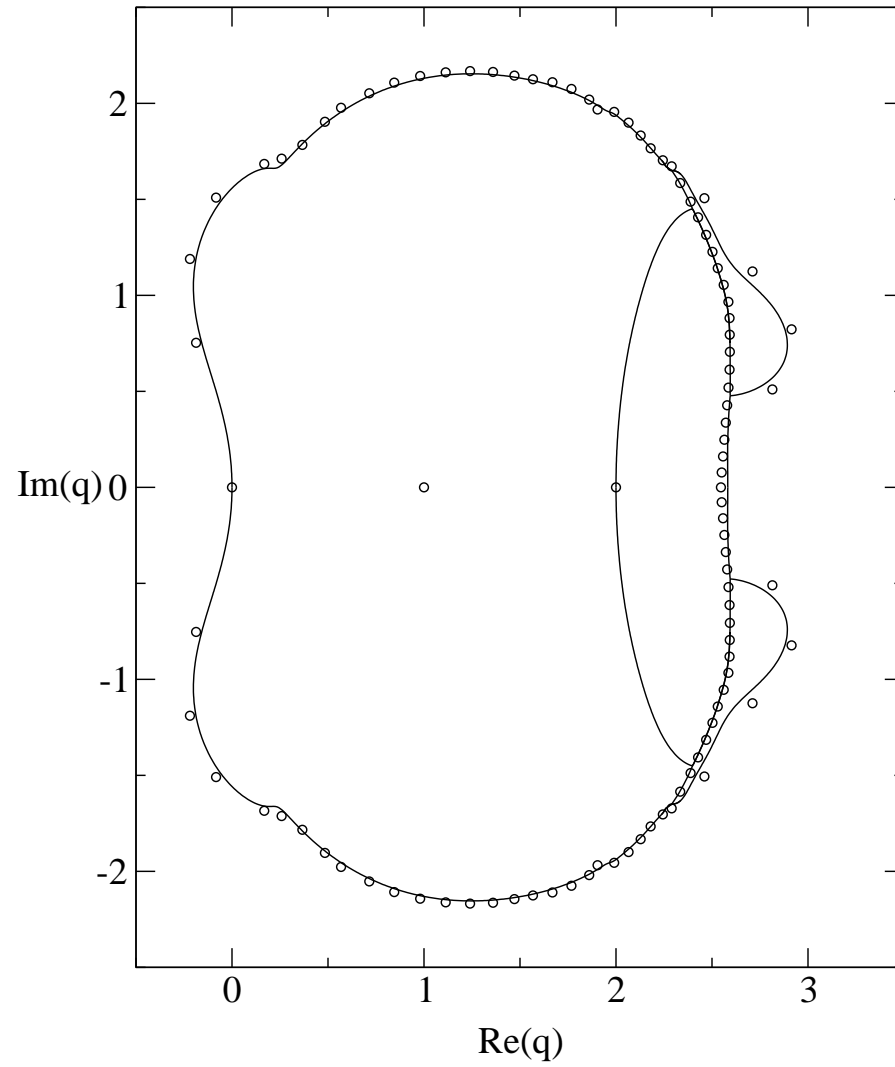


Figure 6: Locus  $\mathcal{B}_q$  for the  $L_x \rightarrow \infty$  limit of the cyclic or Möbius strip of the square lattice of width  $L_y = 5$ . For comparison, chromatic zeros calculated for the cyclic strip with  $L_x = 20$  and thus  $n = 100$  vertices are shown. From S.-C. Chang and R. Shrock, *Physica A* 316, 335 (2002).

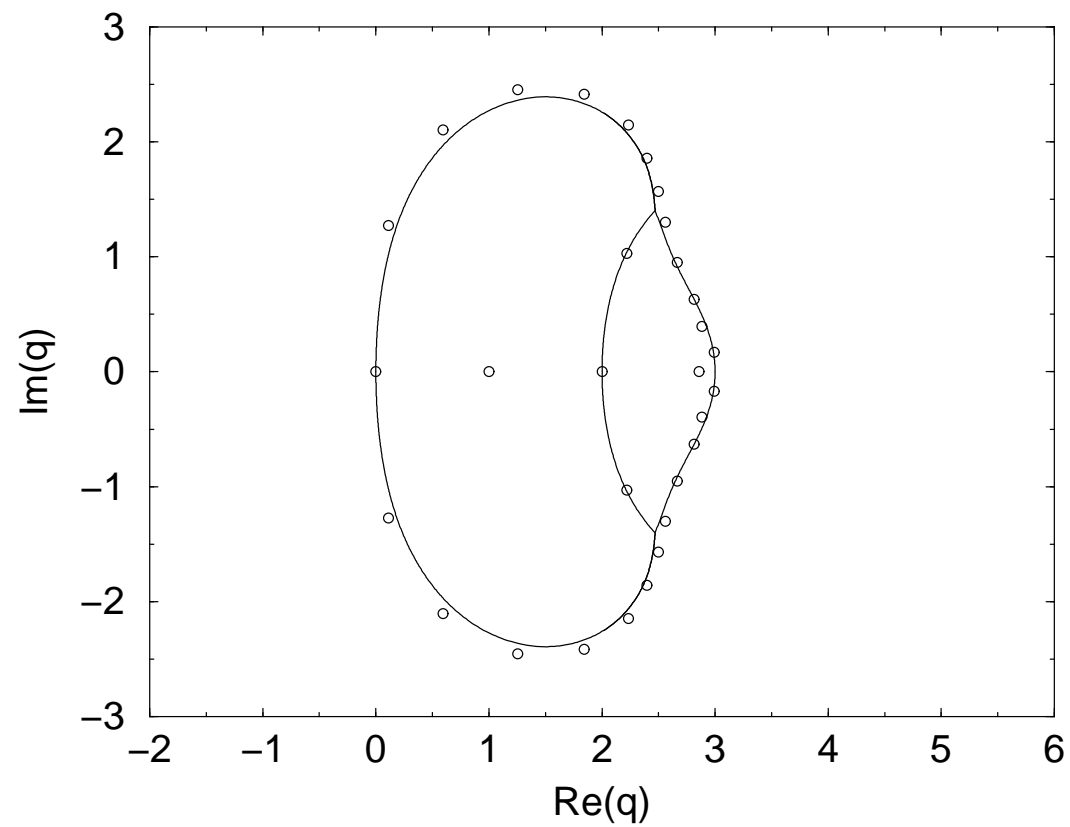


Figure 7: Locus  $\mathcal{B}_q$  for the  $L_x \rightarrow \infty$  limit of the strip of the square lattice with toroidal or Klein Bottle boundary conditions, of width  $L_y = 3$ , with chromatic zeros for a finite  $L_x$  shown for comparison; see N. Biggs and R. Shrock, J. Phys. A (Letts) 32, L489 (1999).

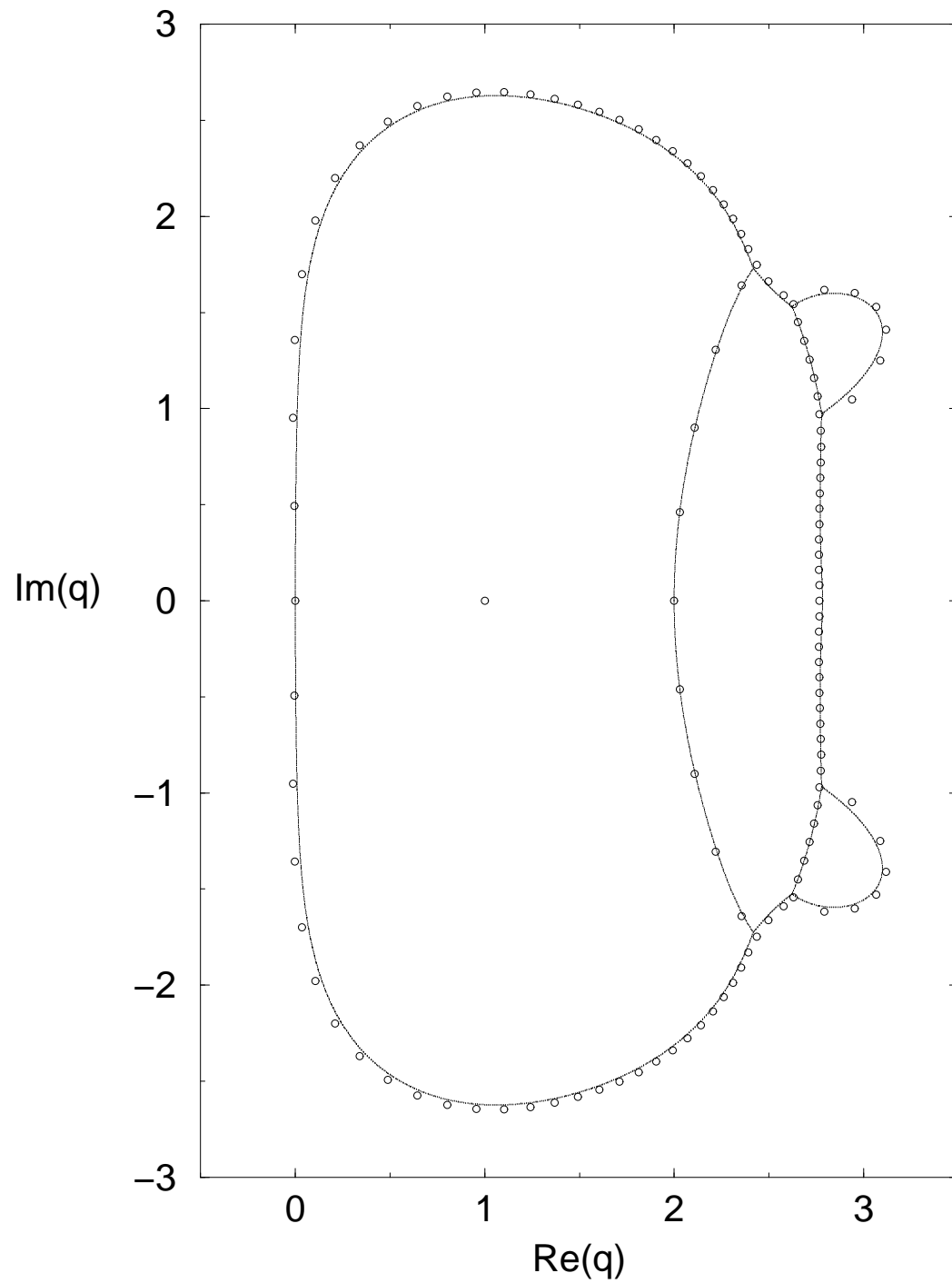


Figure 8: Locus  $\mathcal{B}_q$  for the  $L_x \rightarrow \infty$  limit of the strip of the square lattice with toroidal or Klein bottle boundary conditions, of width  $L_y = 4$ , with chromatic zeros for a finite  $L_x$  shown for comparison, from S.-C. Chang and R. Shrock, Physica A292, 307 (2001).



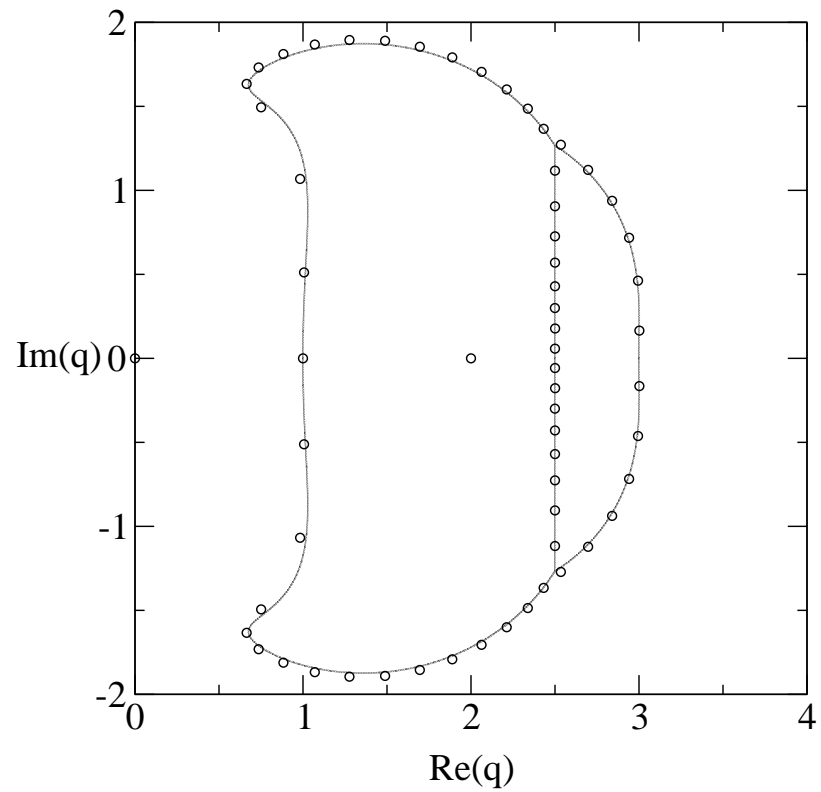


Figure 9: Locus  $\mathcal{B}_q$  for the  $L_x \rightarrow \infty$  limit of  $G_D(2 \times L_x)$ . For comparison, chromatic zeros are shown for  $L_x = 30$ , i.e.,  $n = 61$ . For the  $L_x \rightarrow \infty$  limit of the wheel graph  $G_D(1 \times L_x)$ ,  $\mathcal{B}$  is the circle  $|q - 2| = 1$ . This figure and the others on  $G_D$  strips are from S.-C. Chang and R. Shrock, Physica A301, 301 (2001).

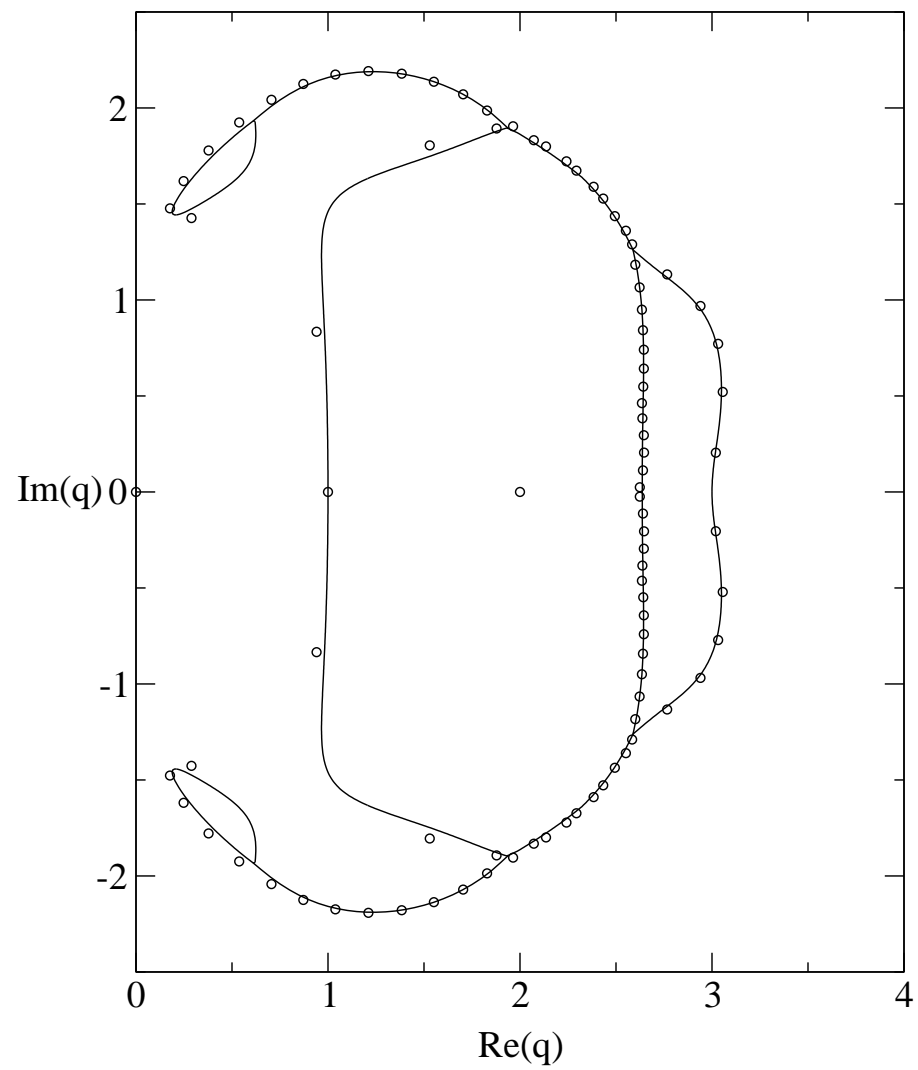


Figure 10: Locus  $\mathcal{B}_q$  for the  $L_x \rightarrow \infty$  limit of  $G_D(3 \times L_x)$ . For comparison, chromatic zeros are shown for  $L_x = 30$ , i.e.,  $n = 91$ .

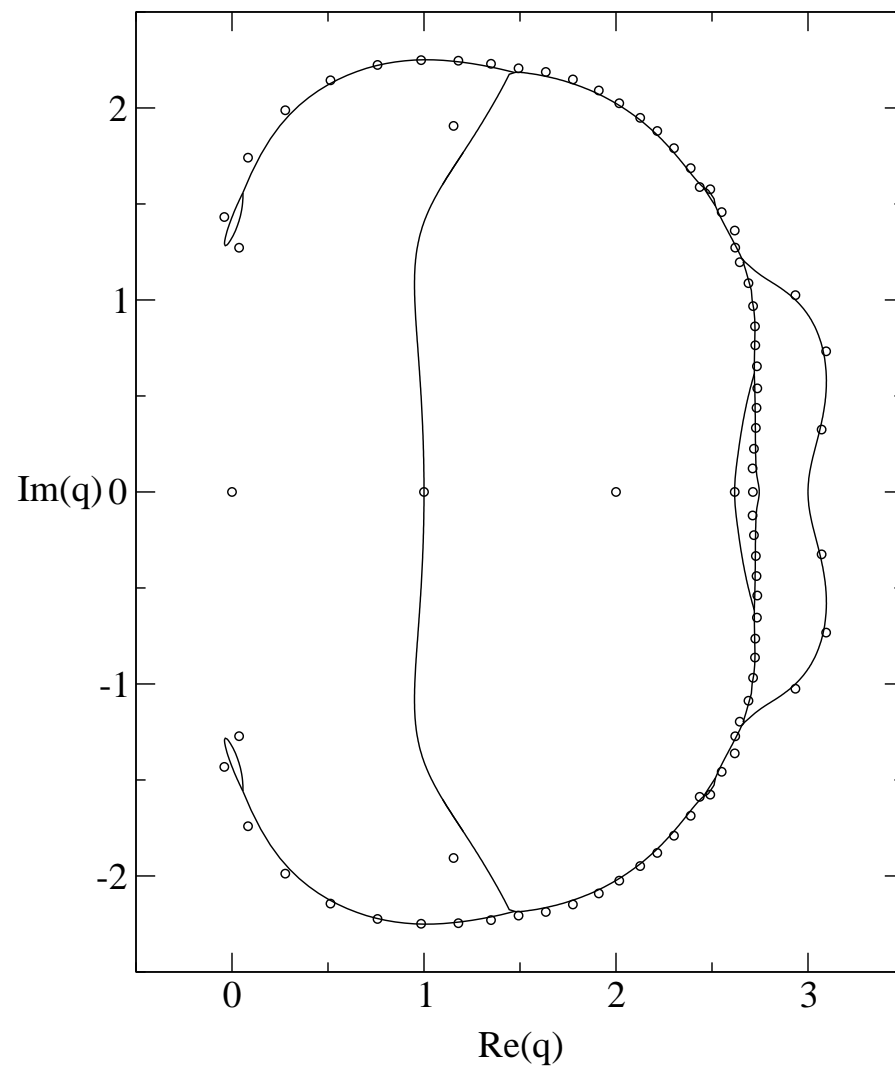


Figure 11: Locus  $\mathcal{B}_q$  for the  $L_x \rightarrow \infty$  limit of  $G_D(4 \times L_x)$ . For comparison, chromatic zeros are shown for  $L_x = 20$ ,  $n = 81$ .

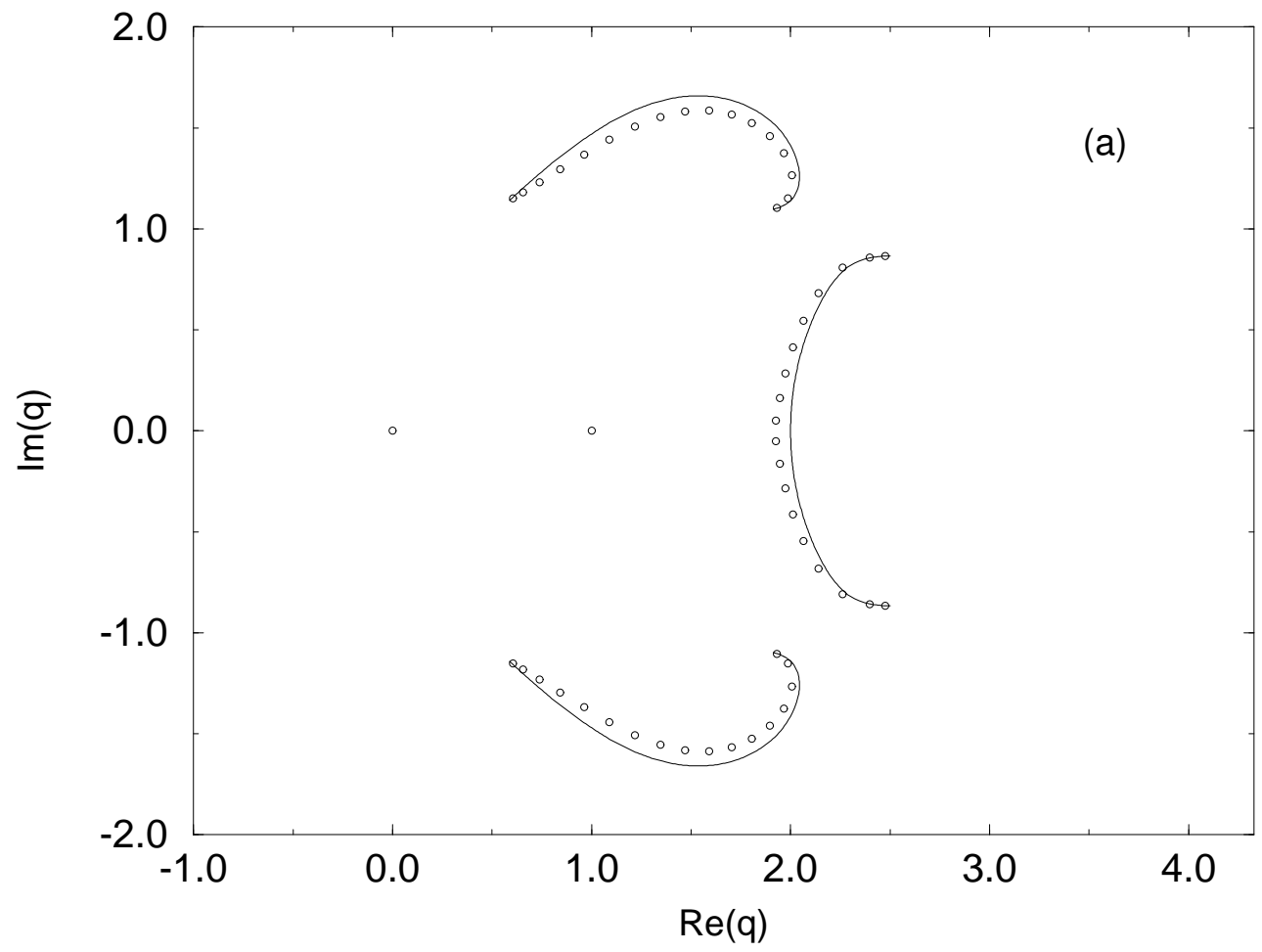


Figure 12: Locus  $\mathcal{B}_q$  for the  $L_x \rightarrow \infty$  limit of the square-lattice strip of width  $L_y = 3$  with free boundary conditions, together with chromatic zeros on a finite- $L_x$  strip shown for comparison. From M. Roček, R. Shrock, and S.-H. Tsai, *Physica A*252, 505 (1998).

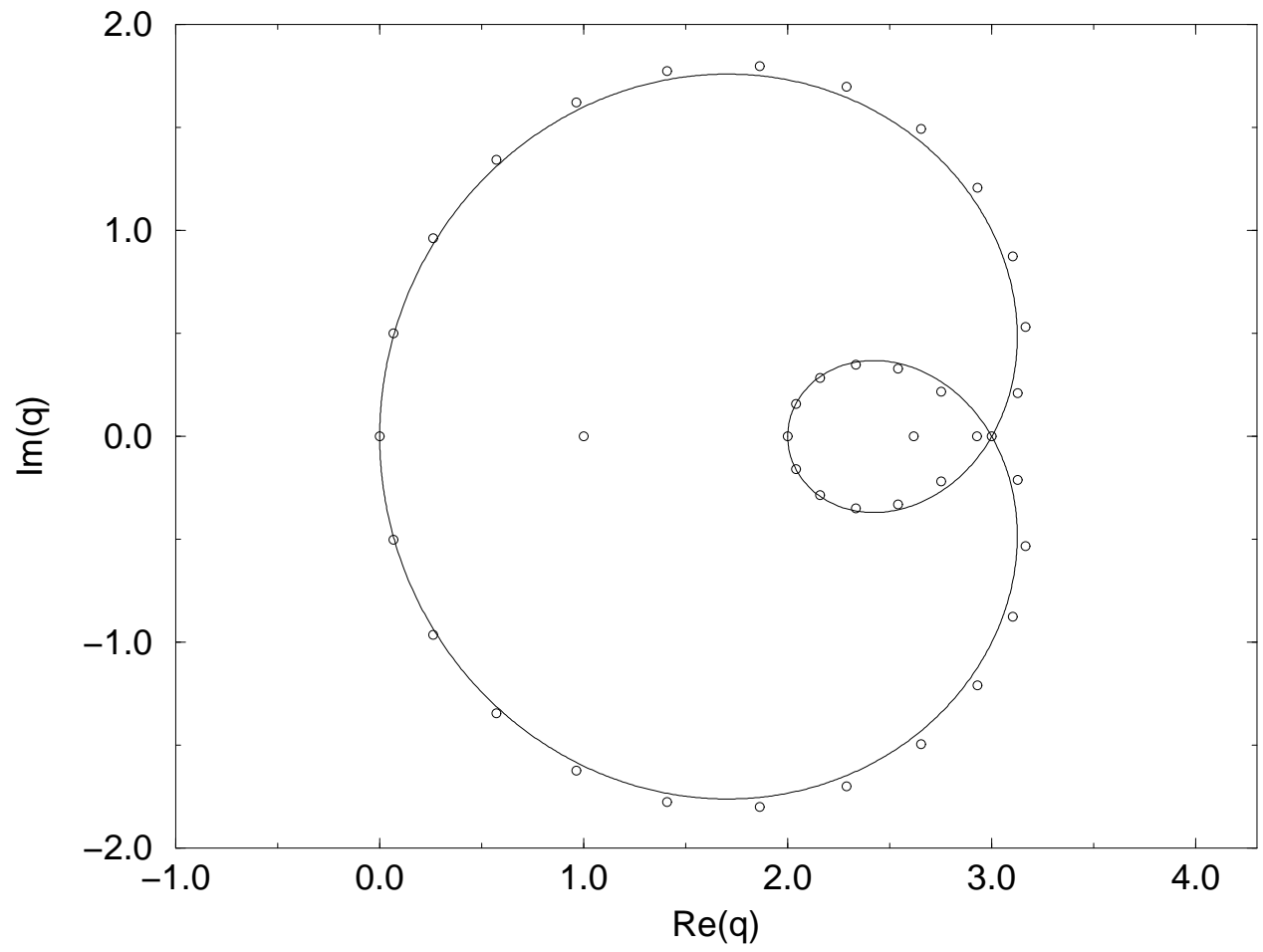


Figure 13: Boundary  $\mathcal{B}_q$  for the  $L_x \rightarrow \infty$  limit of the cyclic or Möbius strip of the triangular lattice with width  $L_y = 2$ . Chromatic zeros for the cyclic strip with  $L_x = 20$  and thus  $n = 40$  vertices are shown for comparison. From R. Shrock and S.-H. Tsai, Physica A275, 429 (2000).

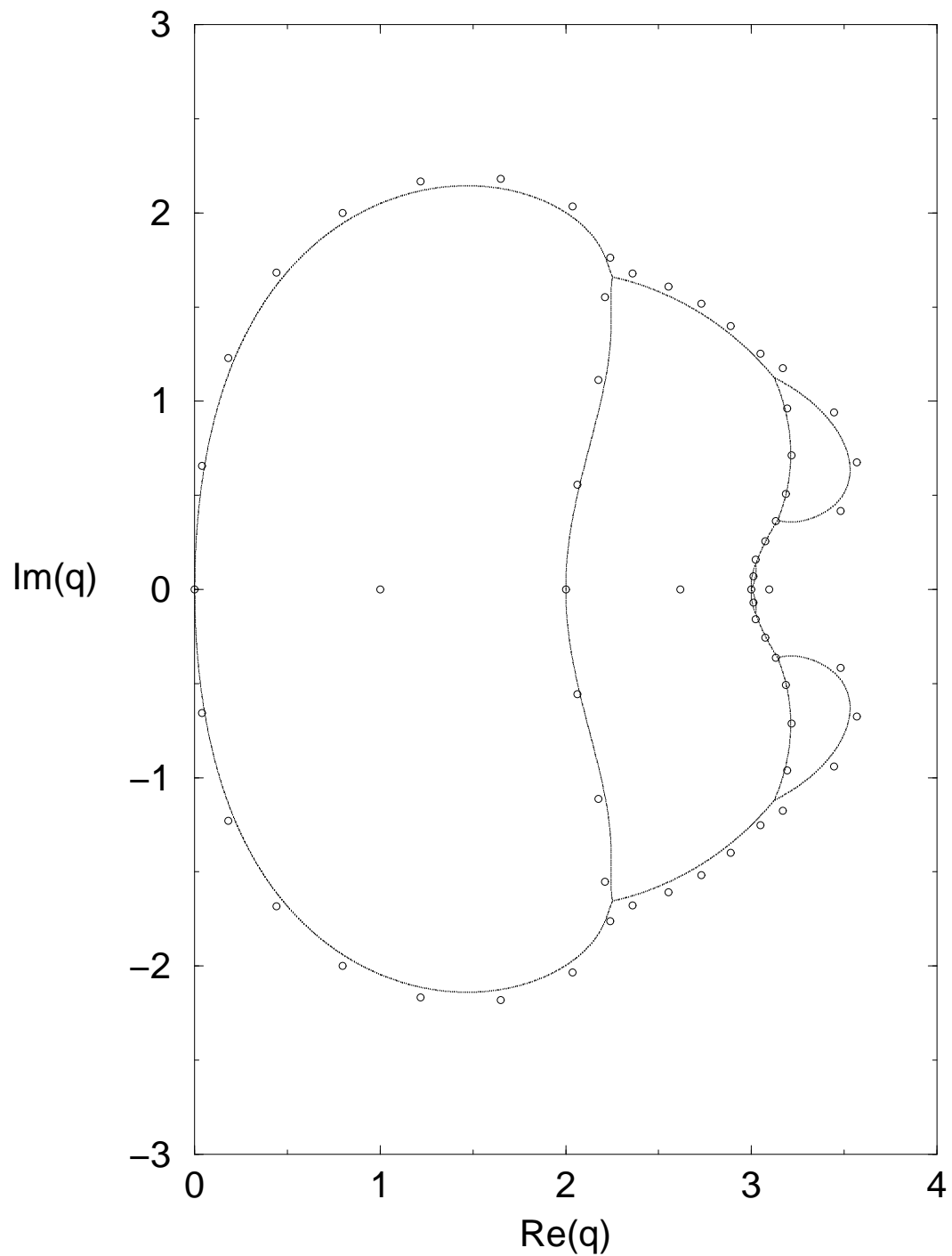


Figure 14: Locus  $\mathcal{B}_q$  for the  $L_x \rightarrow \infty$  limit of the cyclic or Möbius strip of the triangular lattice with width  $L_y = 3$ . Chromatic zeros for the cyclic strip with  $L_x = 20$  and thus  $n = 60$  vertices are shown for comparison. From S.-C. Chang and R. Shrock, Ann. Phys. 290, 124 (2001).

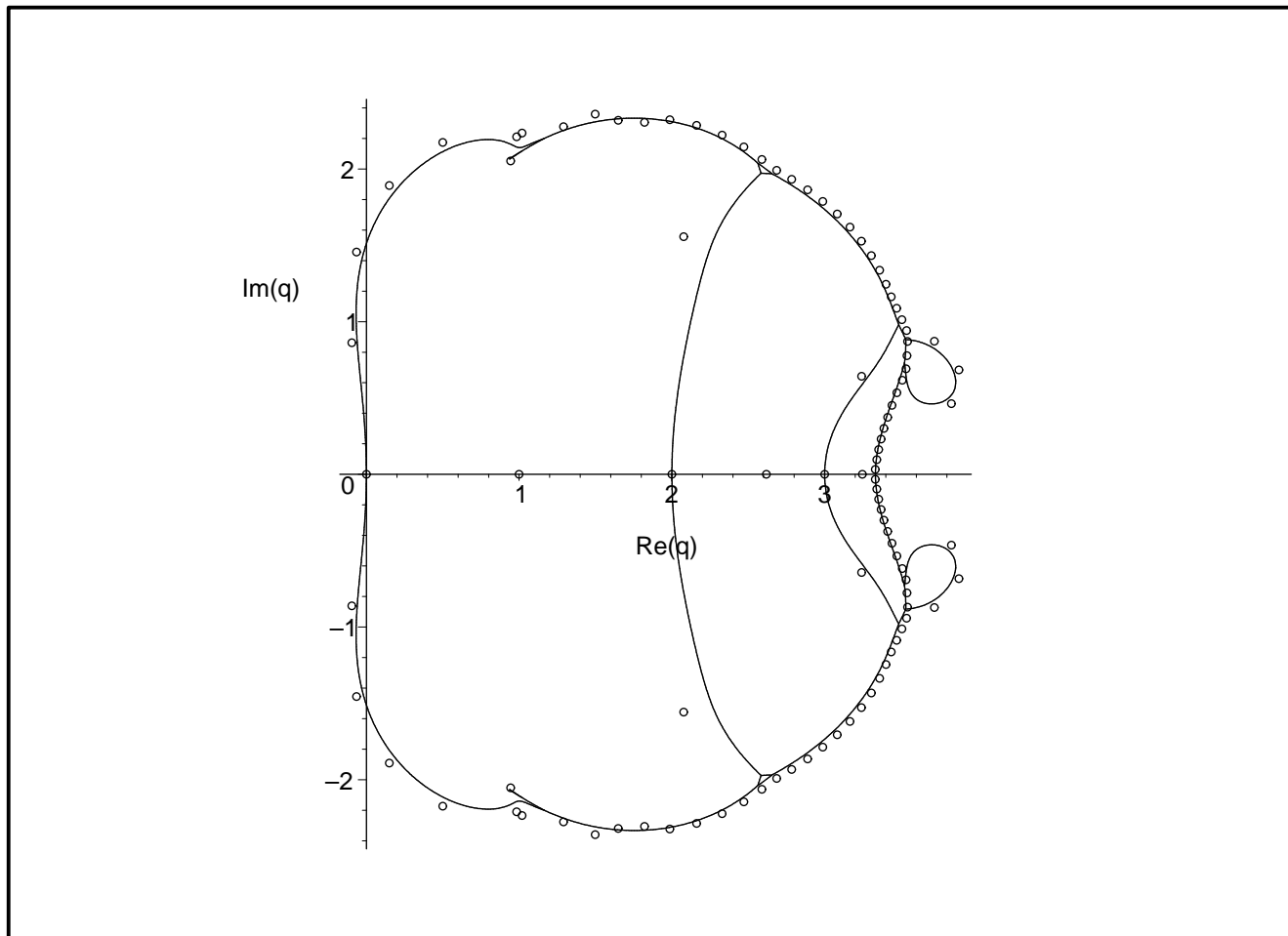


Figure 15: Locus  $\mathcal{B}_q$  for the  $L_x \rightarrow \infty$  limit of the cyclic or Möbius strip of the triangular lattice with width  $L_y = 5$ . Chromatic zeros for the cyclic strip with  $L_x = 20$  and thus  $n = 100$  vertices are shown for comparison. From S.-C. Chang and R. Shrock, *Physica A* 346, 400 (2005).

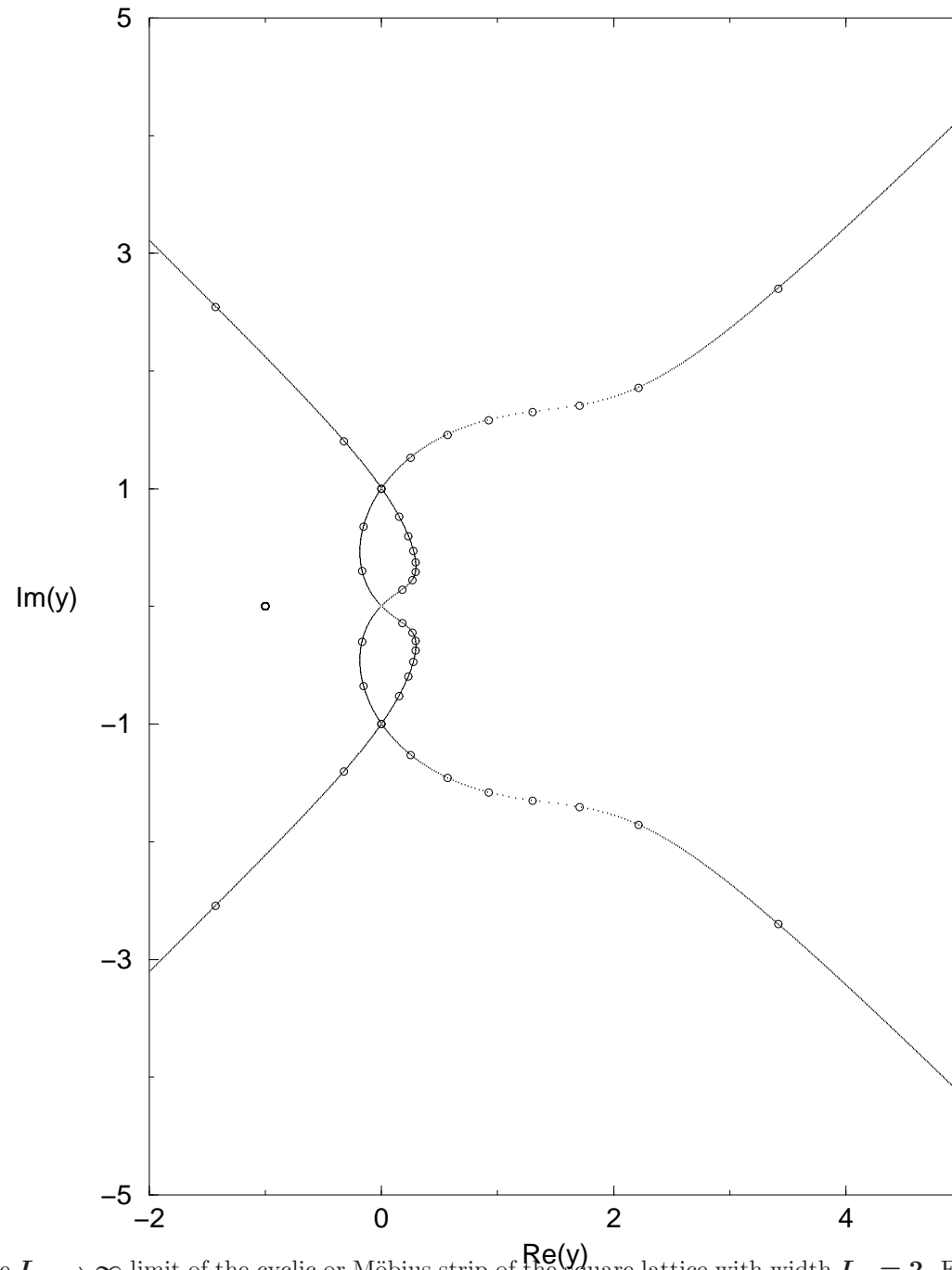


Figure 16: Locus  $\mathcal{B}_y$  for  $q = 2$  in the  $L_x \rightarrow \infty$  limit of the cyclic or Möbius strip of the square lattice with width  $L_y = 2$ . From S.-C. Chang and R. Shrock, *Physica A* 286, 189 (2000).



## Potts Model on Hierarchical Lattices

In the theory of phase transitions and critical phenomena, the renormalization group (RG) has played a very important role (K. Wilson, M. Fisher, A. Migdal, L. Kadanoff..).

Real-space RG: apply blocking transformation with blocking factor  $b$ ; calculate effective Hamiltonian after blocking. Iterating this generates an RG flow in the space of couplings. Calculate fixed points of this RG mapping (RGFPs).

Two general RGFPs:

- infinite-temp. RGFP,  $T = \infty$ ,  $\beta = 1/(k_B T) = 0$ , so  $K = 0$ ,  $v = e^K - 1 = 0$ , i.e.,  $y = v + 1 = 1$ . Here, the spin-spin interaction plays no role, Boltzmann factor  $e^{-\beta \mathcal{H}} = 1$ , and  $Z(G, q, 0) = q^n \forall G$ ; spins are completely disordered; paramagnetic (PM) behavior
- zero-temp. RGFP,  $T = 0$ ,  $\beta = \infty$  and  $v = \infty$  if  $J > 0$  (FM) or  $v = -1$  if  $J < 0$  (AFM) case.
- An RGFP can also occur at finite temperature, with associated critical exponents.

An appeal of hierarchical lattice graphs is that one has an exact closed-form RG transformation.

Examples of hierarchical (lattice) graphs  $G_m$ : Sierpinski triangle  $S_m$ , Diamond hierarchical lattice (DHL) graphs,  $D_m$ . In each case, one starts with a given graph  $G_m$  and iteratively constructs  $G_{m+1}$  by a specified procedure of adding vertices and edges; see figure.

Earlier, we studied zeros of  $Z(S_m, q, v)$  on  $m$ 'th iterates of the Sierpinski graph, for which one has an exact RG transformation for  $Z$  (Chang and RS, Phys. Lett. A377, 671 (2013)).

The Diamond hierarchical lattice is of particular interest: many studies of zeros in  $v$  (and  $w = e^h$  if one includes an external magnetic field), e.g., Gefen, Mandelbrot, and Aharony, 1979-1984; Griffiths and Kaufman, 1981-1982; Derrida, De Seze, Itzykson, 1983; Bleher, Zaly, 1989; Bleher, Lyubich, 1991; Qin- Z. Yang, 19921; Qiao, Gao-Qiao 2001-2011; Bleher, Lyubich, Roeder, BLR1: Lee-Yang Zeros for DHL..., J. Math. Pure Appl. 107, 491 (2017) [ arXiv:1009.4691]; BLR2: Lee-Yang-Fisher Zeros for DHL..., J. Geom. Anal. 30, 777 (2020) [arXiv:1107.5764].

Although there have been studies of zeros in  $v$  and  $w$ , there has been much less work on zeros in  $q$ , including chromatic zeros (for  $v = -1$ ) and zeros in  $q$  for other values of  $v$ . Some recent work: I. Chio and R. Roeder arXiv:1904.02195 (talk by Chio at this workshop) and S.-C. Chang, R. Roeder, and RS, J. Math. Phys. 61, 073301 (2020).

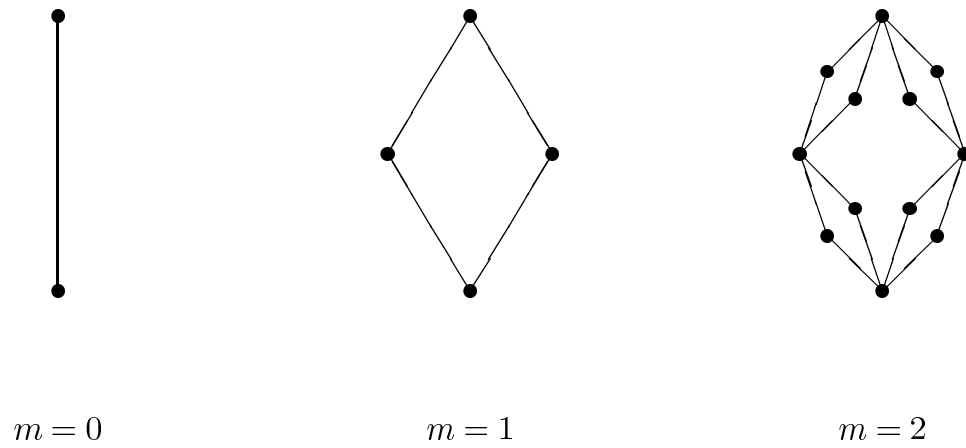


Figure 17: First few iterates  $D_m$  of the Diamond hierarchical lattice.

The  $D_m$  iterate has  $n(D_m) = (2/3)(4^m + 2)$  and  $e(D_m) = 4^m$ .  $D_m$  with  $m \geq 2$  has vertices with degree 2 and 4 and hence is not  $\Delta$ -regular, but, defining effective  $\Delta_{eff} = 2e(G)/n(G)$ , the limit  $\lim_{m \rightarrow \infty} \Delta_{eff}(D_m) = 3$ .

Hausdorff dimension  $d_H$ : each iteration reduces the length of an edge by blocking factor  $b$  and produces  $N$  copies, so  $N = b^{d_H}$ ; here  $b = 2$  and  $N = 4$  so  $d_H(D_\infty) = 2$ .

Since  $D_m$  is bipartite, for  $P(D_m, q)$  it follows that  $P(D_m, 2) = 2$ . We calculate

$$P(D_m, 3) = 2 \cdot 3^{n(D_m)/2}, \quad \implies \quad W(D_\infty, 3) = \sqrt{3}, \quad S_0(D_\infty)/k_B = \frac{1}{2} \ln 3$$

By carrying out the summation over the spins at intermediate vertices at each stage, one finds the exact RG transformation

$$Z(D_{m+1}, q, v) = Z(D_m, q, v')(q + 2v)^{2^{2m+1}}$$

where  $Z(D_0, q, v) = q(q + v)$  and

$$v' = \frac{v^2(2q + 4v + v^2)}{(q + 2v)^2} \equiv F_q(v)$$

or equivalently, with  $y = v + 1$

$$y' = \left[ \frac{q + y^2 - 1}{q + 2(y - 1)} \right]^2 \equiv r_q(y)$$

In the temperature variable  $v$ , the fixed points of this RG mapping occur at  $F_q(v) = v$ :

- the  $T = \infty$  RGFP at  $v = v' = 0$
- the  $T = 0$  RGFP:  $v = \infty$  if  $J > 0$  (FM);  $v = -1$  if  $J < 0$  (AFM)
- depending on  $q$ , a possible finite-temp. RGFP at value of  $v$  given by physical solution of eq.  $v^3 - 2qv - q^2 = 0$ . e.g., for  $q = 2$  (Ising) case, there is a PM-FM phase transition at  $v = v_{c,PM-FM} = 2.3830$  (the other two solutions of the cubic form a complex-conjugate pair, not physical).

For  $q > 32/27 = 1.185185\dots$ , the PM-FM phase transition occurs at

$$v_{c,PM-FM} = 2^{-1/3} \left[ q^2 + \sqrt{q^3(q - (32/27))} \right]^{1/3} + \frac{2^{4/3} q}{3 \left[ q^2 + \sqrt{q^3(q - (32/27))} \right]^{1/3}}$$

Hence,  $v_{c,PM-FM} \sim q^{2/3}$  as  $q \rightarrow \infty$ . This is physically understandable since the larger  $q$  is, the more intrinsic disorder there is in the spin system, and hence the lower the temperature (i.e., the larger  $v = e^K - 1$ ) that one must cool the system to before one gets a nonzero magnetization.

For  $q = 32/27$ , the cubic factorizes as  $[v - (16/9)][v + (8/9)]^2 = 0$ , so the model has a PM-FM critical point at  $v = v_{c,PM-FM} = (4/3)^2$  and an PM-AFM critical point at  $v = v_{c,PM-AFM} = -8/9$  (See our paper for discussion of other  $q$  values.)

The RG transformation with blocking parameter  $b$  takes spin-spin correlation length  $\xi \rightarrow \xi/b$  and hence RGFPs have  $\xi = 0$  (for  $T = \infty$  and  $T = 0$  fixed points) or  $\xi = \infty$  (for finite-temp. PM-FM or PM-AFM second-order phase transitions ).

Since RG block-spin transformation reduces  $\xi$ , it follows that the  $T = \infty$  and  $T = 0$  RGFPs are stable, while a finite-temp. RGFP is unstable under this transformation (so the associated locus  $\mathcal{B}_v$  defined as the accumulation set of zeros in the  $m \rightarrow \infty$  limit is the Julia set of the RG transformation  $v \rightarrow F_q(v)$ ).

Next, we focus on the zeros in the  $q$  plane and their accumulation set in the limit  $m \rightarrow \infty$ , i.e., the locus  $\mathcal{B}_q$ . We have studied this for both  $v = -1$  (chromatic zeros, i.e., Potts AFM at  $T = 0$ ),  $v \in (-1, 0]$  (Potts AFM with temp.  $T > 0$ ), and  $v \geq 0$  (Potts FM).

Figures show region diagrams depending on behavior of  $F_q^m(v)$  and  $q$ -plane zeros for  $Z_r(D_5, q, v)$ :

- regions in  $q$  such that  $F_q^m(-1) \rightarrow 0$  are colored white
- regions in  $q$  such that  $F_q^m(-1) \rightarrow \infty$  are colored blue
- regions in  $q$  not in either of these are colored black

- Similarly to the way the locus  $\mathcal{B}_q$  separated regions with different behavior for the infinite-length strip graphs, here the locus  $\mathcal{B}_q$  consists of points on the boundaries between white, blue, and black regions.

Some properties of  $\mathcal{B}_q$  (more sophisticated discussion using complex dynamics by R. Roeder in CRS paper):

- The left-most point where  $\mathcal{B}_q$  intersects the real  $q$  axis is at  $q = 0$
- The maximal (right-most) value at which  $\mathcal{B}_q$  crosses the real axis is at  $q_c = 3$ . (However,  $P(D_m, 3)$  is nonzero, equal to  $2 \cdot 3^{n(D_m)/2}$ .)
- The minimal nonzero value of  $q$  at which  $\mathcal{B}_q$  crosses the real axis is at  $q = 32/27 = 1.185185\dots$  (although  $1 < q \leq 32/27$  is a chromatic zero-free region for any  $P(G, q)$  [Jackson, Thomassen])
- Moving left from  $q_c$ ,  $\mathcal{B}_q$  crosses the real axis at an infinite sequence of points given by solutions to  $F_q^m(-1) = F_q(-1)$ ,  $m \geq 2$ , starting with a solution to  $F_q^2(-1) = F_q(-1)$ ,  $q = 1.638897\dots$ , (unique real root of the equation  $q^3 - 5q^2 + 11q - 9 = 0$ ), converging to  $q = 32/27$  from above.

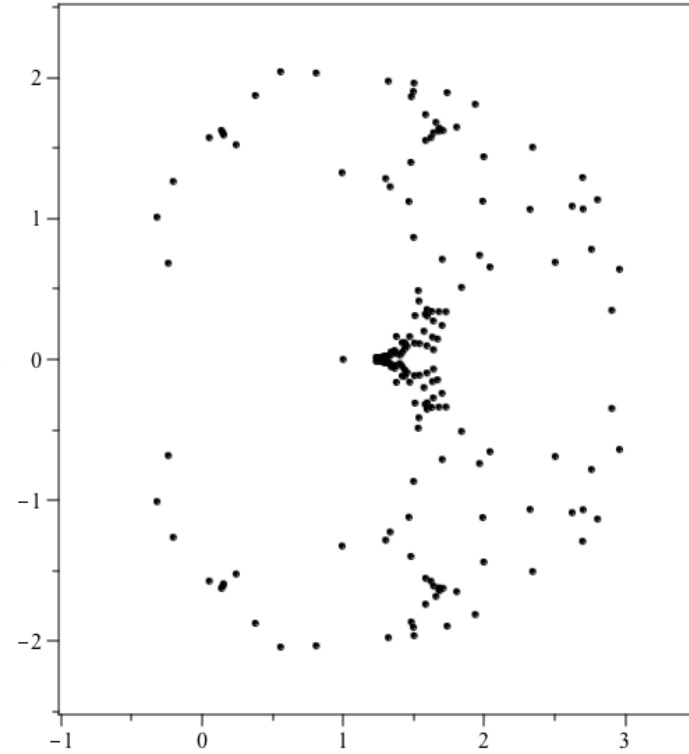
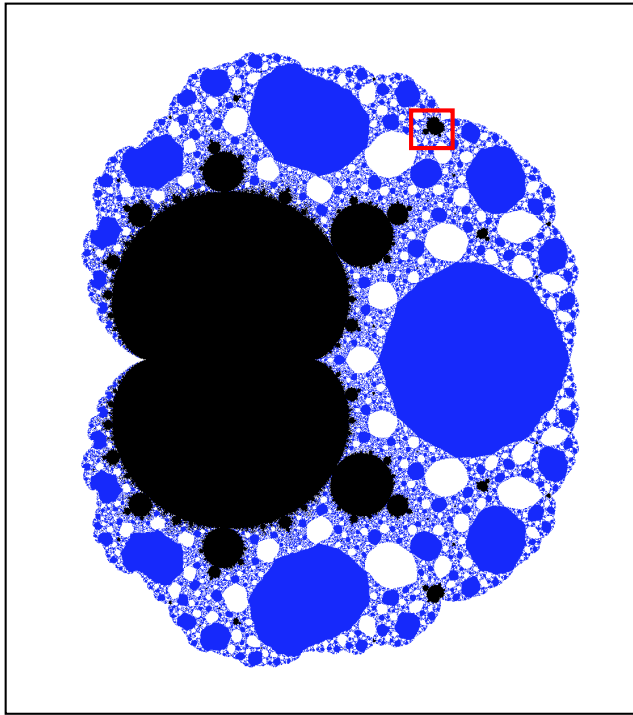


Figure 18: Locus  $\mathcal{B}_q$  for  $D_\infty$  DHL lattice and  $v = -1$  (R. Roeder), together with chromatic zeros of  $P_r(D_5, q)$ . In both panels, the real and imaginary intervals are  $-1 < \text{Re}(q) < 3.5$  and  $-2.5 < \text{Im}(q) < 2.5$ .



We proceed to discuss  $\mathcal{B}_q$  for  $v > -1$ . As  $v$  increases in the interval  $-1 < v < 0$ , the locus  $\mathcal{B}_q$  shrinks, and more of the interior is black. As  $v \rightarrow 0^-$ ,  $\mathcal{B}_q$  degenerates to a single point  $q = 0$ , since  $Z(G, q, 0) = q^n$  for any  $G$ .

For  $v > 0$ ,  $\mathcal{B}_q$  crosses the real axis at only two points.

As  $v$  increases from 0 through positive real values (Potts ferromagnet), the black and white regions in the interior of the outermost part of  $\mathcal{B}_q$  are reduced, with the blue regions becoming dominant.

For large real positive  $v$  (Potts ferromagnet at low temperature),  $\mathcal{B}_q$  becomes more like a roughly circular curve, with radius  $|q| \sim v^{3/2}$ , corresponding to the solution for  $v_{c,PM-FM}$  above, and the interior of  $\mathcal{B}_q$  becomes blue.

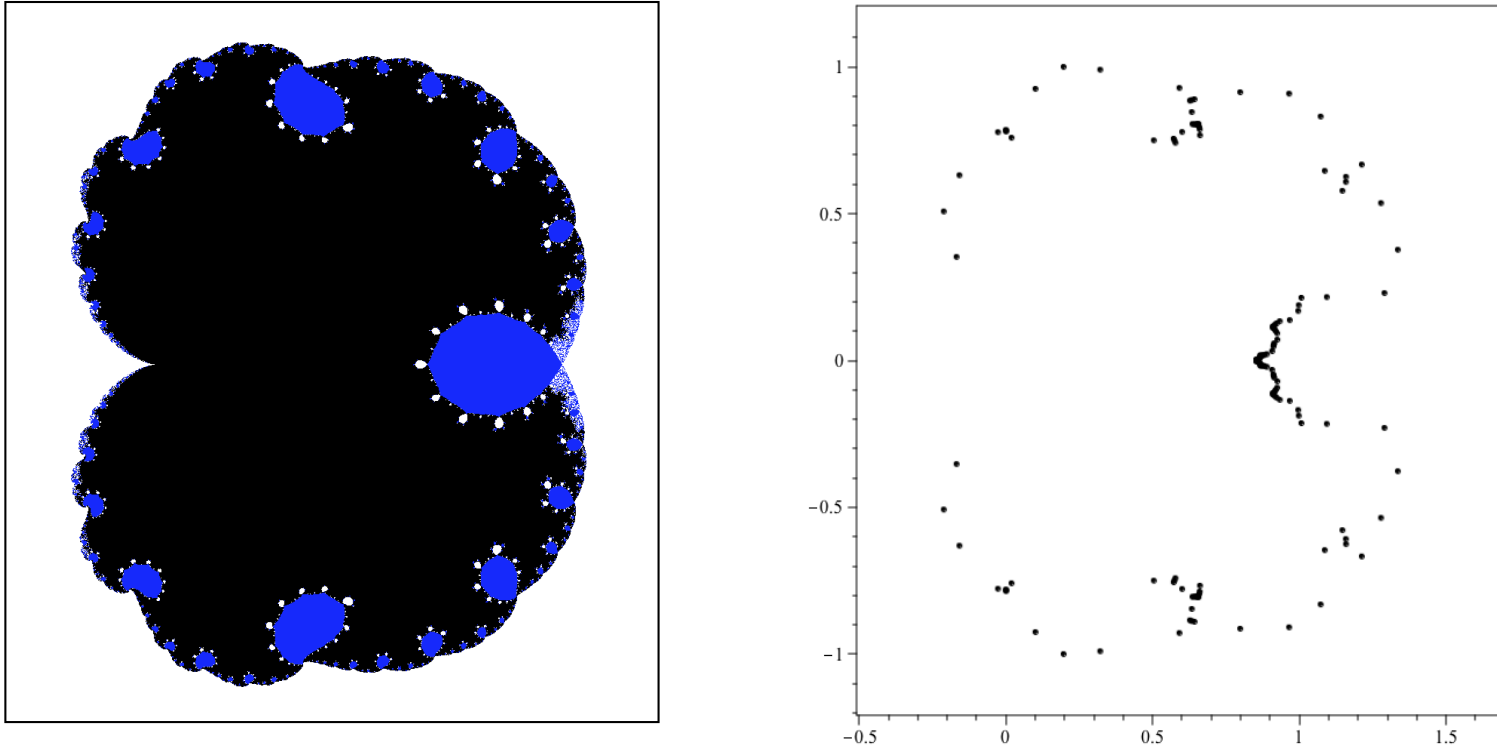


Figure 19: Locus  $\mathcal{B}_q$  for  $D_\infty$  with  $v = -0.5$ , together with zeros of  $Z_r(D_5, q, -0.5)$ . In both panels, the real and imaginary intervals are  $-0.5 < \text{Re}(q) < 1.7$  and  $-1.2 < \text{Im}(q) < 1.2$ . This and other figs. from CRS.

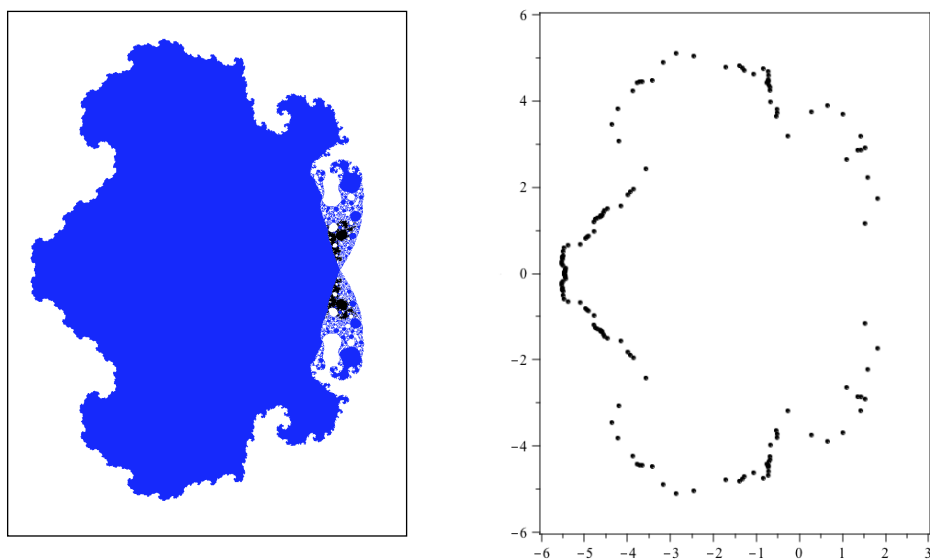


Figure 20: Locus  $\mathcal{B}_q$  for  $D_\infty$  with  $v = 2$ , together with zeros of  $Z_r(D_5, q, 2)$ . In both panels, the real and imaginary intervals are  $-6 < \text{Re}(q) < 3$  and  $-6 < \text{Im}(q) < 6$ .

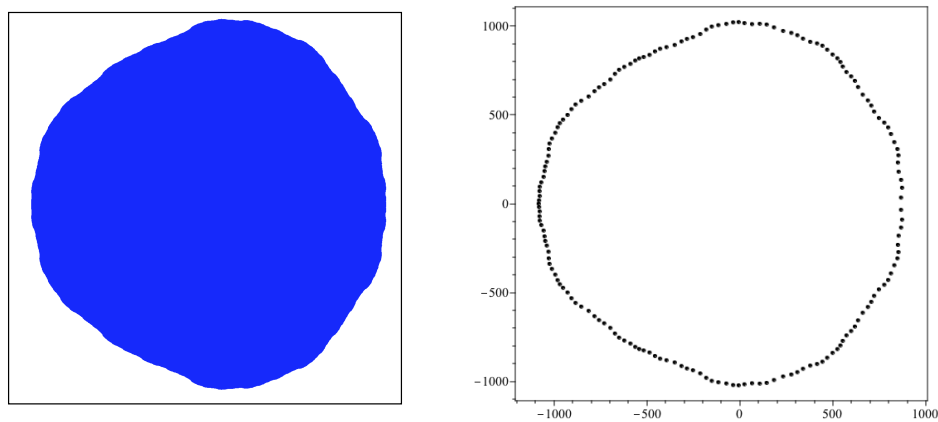


Figure 21: Locus  $\mathcal{B}_q$  for  $D_\infty$  with  $v = 99$  (i.e.,  $y = 100$ ), together with zeros of  $Z_r(D_5, q, 99)$ . In both panels, the real and imaginary intervals are  $-1200 < \text{Re}(q) < 1000$  and  $-1100 < \text{Im}(q) < 1100$ .

# Some Open Problems and Directions for Further Research

There are many open problems and directions for further research, e.g.,

1. Further calculations of  $Z(G, q, v)$  and  $P(G, q)$  for various families of graphs, with analysis of zeros and the accumulation sets  $\mathcal{B}_v$  at fixed  $q$  and  $\mathcal{B}_q$  at fixed  $v$ , as well as analogous loci if one imposes a functional relation  $\omega(v, q) = 0$ .
2. We have found that, for infinite-length lattice strips with arbitrary transverse boundary conditions, a sufficient condition for  $\mathcal{B}_q$  to separate the complex  $q$  plane into regions is that the longitudinal b.c. should be periodic or twisted periodic (cyclic, Möbius, toroidal, or Klein-bottle). Prove this in general.
3. In all of the infinite-length limits of families of graphs with cyclic boundary conditions, we have found that  $q_c$  is a nondecreasing function of  $L_y$ . Prove this in general. Note that we have shown that this monotonicity does not hold for infinite-length limits of graphs with toroidal or Klein-bottle boundary conditions.
4. For the infinite-length limits of families of graphs for which  $\mathcal{B}_q$  does separate the complex  $q$  plane into several regions, give a precise characterization of the number of regions. This is related to the Hilbert 16'th problem, to determine the topology of solutions to algebraic equations. In specific cases, e.g.,  $m \rightarrow \infty$  limit of a necklace graph (RS and Tsai, J. Phys. A 32, 5053 (1999)) the number of disjoint curves and associated regions that we find is much less than the Harnack upper bound.

5. Analyze  $\mathcal{B}_v$  and  $\mathcal{B}_w$  for DHL with values of  $q$  other than the Ising case  $q = 2$ .
6. Further study of  $\mathcal{B}_q$  for DHL with  $v > -1$ , including both the  $J < 0$  regime  $-1 < v \leq 0$  and the  $J > 0$  regime,  $v \geq 0$ .
7. Study the loci  $\mathcal{B}_q$  and  $\mathcal{B}_v$  for other hierarchical lattices.

## Conclusions

- Interesting connections between the Potts model in statistical mechanics and the Tutte polynomial.
- $T = 0$  Potts antiferromagnet partition function is identical to the chromatic polynomial relevant for graph coloring.
- Worthwhile to study pattern of zeros of  $Z(G, q, v)$  in  $v$  plane for fixed  $q$  and in  $q$  plane for fixed  $v$ . For infinite-length limits of strip graphs, these zeros merge to form curves. At points where these cross the real  $q$  or  $v$  axes,  $f$  and  $W$  functions change analytic form.
- Connection with ground entropy of zero-temperature Potts AFM
- We have calculated these curves for several infinite-length limits of lattice strips for various lattice types, widths, and boundary conditions.
- Valuable insights from study (with S.-C. Chang and R. Roeder) of  $\mathcal{B}_q$  on the Diamond Hierarchical Lattice.
- Thus, study of the properties of the Potts/Tutte and chromatic polynomials for these families of graphs, including the asymptotic behavior as  $n \rightarrow \infty$ , involves interesting confluence of physics and mathematics.
- Many open questions that could be investigated in future work

Thank you to Roland Roeder for a very instructive collaboration and for inviting me to give this talk.

Thank you also to the audience.

## Some of our Papers on Potts, Tutte, and Chromatic Polynomials

1. V. Matveev and R. Shrock, “Complex-Temperature Singularities of the Susceptibility in the  $d = 2$  Ising Model: Square Lattice”, J. Phys. A 28, 1557-1583 (1995) [hep-lat/9408020].
2. V. Matveev and R. Shrock, “Complex-Temperature Singularities in the  $d = 2$  Ising Model: Triangular and Honeycomb Lattices”, J. Phys. A 29, 803-823 (1996).
3. V. Matveev and R. Shrock, “Complex-Temperature Properties of the 2D Ising Model on Heteropolygonal Lattices”, J. Phys. A 28, 5235-5256 (1995) [hep-lat/9503005].
4. V. Matveev and R. Shrock, “Complex-Temperature Properties of the 2D Ising Model with  $\beta H = i\pi/2$ ”, J. Phys. A 28, 4859-4882 (1995) [hep-lat/9412105]
5. V. Matveev and R. Shrock, “Complex-Temperature Properties of the 2D Ising Model for Nonzero Magnetic Field”, Phys. Rev. E53, 254-267 (1996).
6. V. Matveev and R. Shrock, “Complex-Temperature Singularities in Potts Models on the Square Lattice”, Phys. Rev. E54, 6174-6185 (1996).
7. V. Matveev and R. Shrock, “Some New Results on Yang-Lee Zeros of the Ising Model Partition Function”, Phys. Lett. A215, 271-279 (1996) [cond-mat/9512149].
8. R. Shrock and S.-H. Tsai, “Asymptotic Limits and Zeros of Chromatic Polynomials and Ground State Entropy of Potts Antiferromagnets” Phys. Rev. E55, 5165-5179 (1997) (cond-mat/9612249).
9. R. Shrock and S.-H. Tsai, “Ground State Entropy and the  $q = 3$  Potts Antiferromagnet on the Honeycomb Lattice”, J. Phys. A 30, 495-500 (1997) (cond-mat/9608095).
10. R. Shrock and S.-H. Tsai, “Upper and Lower Bounds for Ground State Entropy of Antiferromagnetic Potts Models”, Phys. Rev. E55, 6791-6794 (1997) (cond-mat/9701162).
11. R. Shrock and S.-H. Tsai, “Families of Graphs with Chromatic Zeros Lying on Circles”, Phys. Rev. E56, 1342-1345 (1997) (cond-mat/9703249).



12. R. Shrock and S.-H. Tsai, "Ground State Entropy of Potts Antiferromagnets: Bounds, Series, and Monte Carlo Measurements", Phys. Rev. E56, 2733-2737 (1997) (cond-mat/9706162).
13. R. Shrock and S.-H. Tsai, "Families of Graphs with  $W_r(\{G\}, q)$  Functions That Are Nonanalytic at  $1/q = 0$ ", Phys. Rev. E56, 3935-3943 (1997) (cond-mat/9707096).
14. R. Shrock and S.-H. Tsai, "Lower Bounds and Series for the Ground State Entropy of the Potts Antiferromagnet on Archimedean Lattices and their Duals", Phys. Rev. E56, 4111-4124 (1997) (cond-mat/9707306).
15. M. Roček, R. Shrock, and S.-H. Tsai, "Chromatic Polynomials for Families of Strip Graphs and their Asymptotic Limits", Physica A252, 505-546 (1998) (cond-mat/9712148).
16. R. Shrock and S.-H. Tsai, "Ground State Entropy of Potts Antiferromagnets on Homeomorphic Families of Strip Graphs", Physica A259, 315-348 (1998) (cond-mat/9807105).
17. H. Feldmann, R. Shrock, and S.-H. Tsai, "A Mapping Relating Complex and Physical Temperatures in the 2D  $q$ -State Potts Model and Some Applications", J. Phys. A (Lett.) 30, L663-668 (1997) (cond-mat/9710018).
18. R. Shrock and S.-H. Tsai, "Ground State Degeneracy of Potts Antiferromagnets: Cases with Noncompact  $W$  Boundaries Having Multiple Points at  $1/q = 0$ ", J. Phys. A 31, 9641-9665 (1998) (cond-mat/9810057).
19. R. Shrock and S.-H. Tsai, "Ground State Degeneracy of Potts Antiferromagnets: Homeomorphic Classes with Noncompact  $W$  Boundaries", Physica A265, 186-223 (1999) (cond-mat/9811410).
20. R. Shrock and S.-H. Tsai, "Ground State Entropy of the Potts Antiferromagnet on Cyclic Strip Graphs", J. Phys. A Letts. 32, L195-L200 (1999) (cond-mat/9903233).
21. R. Shrock and S.-H. Tsai, "Ground State Entropy of Potts Antiferromagnets on Cyclic Polygon Chain Graphs", J. Phys. A 32, 5053-5070 (1999) (cond-mat/9905431).
22. R. Shrock and S.-H. Tsai, "Ground State Degeneracy of Potts Antiferromagnets on 2D Lattices: Approach Using Infinite Cyclic Strip Graphs", Phys. Rev. E60, 3512-3515 (1999) (cond-mat/9910377).
23. R. Shrock and S.-H. Tsai, "Exact Partition Functions for Potts Antiferromagnets on Cyclic Lattice Strips", Physica A 275, 429-449 (2000) (cond-mat/9907403).

24. R. Shrock, " $T = 0$  Partition Functions for Potts Antiferromagnets on Möbius Strips and Effects of Graph Topology", Phys. Lett. A261, 57-62 (1999) (cond-mat/9908323).
25. N. L. Biggs and R. Shrock, " $T = 0$  Partition Functions for Potts Antiferromagnets on Square Lattice Strips with (Twisted) Periodic Boundary Conditions", J. Phys. A (Letts) 32, L489-L493 (1999) (cond-mat/0001407).
26. R. Shrock, "Chromatic Polynomials and their Zeros and Asymptotic Limits for Families of Graphs", in Proceedings of the 1999 British Combinatorial Conference, BCC99 (July, 1999), Discrete Math. 231, 421-446 (2001) (cond-mat/9908387).
27. R. Shrock, "Exact Potts Model Partition Functions for Ladder Graphs", Physica A 283, 388-446 (2000) (cond-mat/0001389).
28. S.-C. Chang and R. Shrock, "Ground State Entropy of the Potts Antiferromagnet with Next-Nearest-Neighbor Spin-Spin Couplings on Strips of the Square Lattice" Phys. Rev. E 62, 4650-4664 (2000) (cond-mat/0005236).
29. S.-C. Chang and R. Shrock, "Exact Potts Model Partition Functions on Strips of the Triangular Lattice", Physica A 286, 189-238 (2000) (cond-mat/0004181).
30. S.-C. Chang and R. Shrock, "Ground State Entropy of the Potts Antiferromagnet on Strips of the Square Lattice", Physica A 290, 402-430 (2001) (cond-mat/0004161).
31. S.-C. Chang and R. Shrock, "Structural Properties of Potts Model Partition Functions and Chromatic Polynomials for Lattice Strips", Physica A 296, 131-182 (2001) (cond-mat/0005232).
32. R. Shrock and F. Y. Wu, "Spanning Trees on Graphs and Lattices in  $d$  Dimensions", J. Phys. A 33 3881-3902 (2000) [cond-mat/0004341].
33. S.-C. Chang and R. Shrock, " $T = 0$  Partition Functions for Potts Antiferromagnets on Lattice Strips with Fully Periodic Boundary Conditions", Physica A 292, 307-345 (2001) (cond-mat/0007491).
34. S.-C. Chang and R. Shrock, "Exact Potts Model Partition Functions on Strips of the Honeycomb Lattice", Physica A 296, 183-233 (2001) (cond-mat/0008477).
35. S.-C. Chang and R. Shrock, "Exact Potts Model Partition Functions on Wider Arbitrary-Length Strips of the Square Lattice, Physica A 296, 234-288 (2001) (cond-mat/0011503).

36. S.-C. Chang and R. Shrock, "Potts Model Partition Functions for Self-Dual Families of Graphs", *Physica A* 301, 301-329 (2001) (cond-mat/0106607).
37. S.-C. Chang and R. Shrock, "Complex-Temperature Phase Diagrams for the  $q$ -State Potts Model on Self-Dual Families of Graphs and the Nature of the  $q \rightarrow \infty$  Limit", *Phys. Rev. E* 64, 066116 (16 p.) (2001) (cond-mat/0107012).
38. S.-C. Chang, J. Salas, and R. Shrock, "Exact Potts Model Partition Functions for Strips of the Square Lattice" *J. Stat. Phys.* 107 1207-1253 (2002) [cond-mat/0108144].
39. S.-C. Chang and R. Shrock, "Tutte Polynomials and Related Asymptotic Limiting Functions for Recursive Families of Graphs", in *Advances in Applied. Math.* 32, 44-87 (2003) (math-ph/0112061).
40. S.-C. Chang and R. Shrock, "General Structural Results for Potts Model Partition Functions on Lattice Strips", *Physica A* 316, 335-379 (2002) (cond-mat/0201223).
41. S.-C. Chang and R. Shrock, "Flow Polynomials and their Asymptotic Limits for Lattice Strip Graphs", *J. Stat. Phys.*, 112, 815-879 (2003) (math-ph/0205424).
42. S.-C. Chang and R. Shrock, "Reliability Polynomials and their Asymptotic Limits for Lattice Strips", *J. Stat. Physics* 112, 1019-1077 (2003) (cond-mat/0208538).
43. S.-C. Chang and R. Shrock, "Exact Results for Average Cluster Numbers in Bond Percolation on Lattice Strips", *Phys. Rev. E* 70, 056130 (2004) (cond-mat/0407070).
44. S.-C. Chang and R. Shrock, "Some Exact Results for Spanning Trees on Lattices", *J. Phys. A* 39, 5653-5658 (2006) (cond-mat/0602574).
45. V. Matveev and R. Shrock, "On Properties of the Ising Model for Complex Energy/Temperature and Magnetic Field", *J. Phys. A* 41, 135002 (2008) [arXiv:0711.4639].
46. S.-C. Chang and R. Shrock, "Some Exact Results on the Potts Model Partition Function in a Magnetic Field", *J. Phys. A* 42, 385004 (2009) [arXiv:0907.0777].
47. S.-C. Chang and R. Shrock, "Weighted Graph Colorings", *J. Stat. Phys.* 138, 496-542 (2010) [arXiv:0908.2375].
48. R. Shrock and Y. Xu, "Weighted-Set Graph Colorings", *J. Stat. Phys.* 139, 27-61 (2010) [arXiv:0911.4218].

49. R. Shrock and Y. Xu, “Exact Results on Potts Model Partition Functions in a Generalized External Field and Weighted-Set Graph Colorings”, J. Stat. Phys 141, 909-939 (2010) [arXiv:1009.1182].
50. R. Shrock, “Exact Potts/Tutte Polynomials for Polygon Chain Graphs”, J. Phys. A, 44, 145002 (2011) [arXiv:1101.3247].
51. S.-C. Chang and R. Shrock, “Zeros of the Potts Model Partition Function on Sierpinski Graphs” Phys. Lett. A 377, 671-675 (2013) [arXiv:1209.0020].
52. S.-C. Chang and Robert Shrock, “Asymptotic Behavior of Acyclic and Cyclic Orientations of Directed Lattice Graphs”, Physica A 540, 123059 (2020) [ arXiv:1810.07357]
53. S.-C. Chang and Robert Shrock, “Study of Exponential Growth Constants of Directed Heteropolygonal Archimedean Lattices”, J. Stat. Phys. 174, 12881315 (2019) [arXiv:1810.11322].
54. S.-C. Chang, R. K. W. Roeder, and R. Shrock, “ $q$ -Plane Zeros of the Potts Partition Function on Diamond Hierarchical Graphs”, J. Math. Phys. 61, 073301 (2020) [arXiv:1911.04012].
55. S.-C. Chang and Robert Shrock, “Asymptotic Behavior of Spanning Forests and Connected Spanning Subgraphs on Two-Dimensional Lattices”, Int. J. Mod. Phys. B 34, 2050249 (2020) [arXiv:2002.07150].
56. S.-C. Chang and R. Shrock, “Exponential Growth Constants for Spanning Forests on Archimedean Lattices: Values and Comparisons of Upper Bounds”, Int. J. Mod. Phys. B 35, 2150085 (2021) [arXiv:2012.13468].